Analysis of a Metallo-protein, Ribonuclease HI by Native Mass Spectrometry

Tomoshige Ando

Department of Chemistry
Graduate School of Science
Osaka University

2018

Index

Abbreviations

ACN	Acetonitrile
AcOH	Acetic acid
B. halodurans	Bacillus halodurans
Conc.	Concentration
DTT	Dithiothreitol
E.coli	Escherichia coli
EDTA	Ethylenediaminetetraacetic acid
ESI	Electrospray ionization
HIV	Human Immunodeficiency Virus
LB	Luria-Bertani
MALDI	Matrix assisted laser desorption ionization
MS	Mass spectrometry
NH_4OAc	Ammonium acetate
OVA	Ovalbumin
RNase H	Ribonuclease H
RT	Reverse transcriptase
SEC	Size-exclusion chromatography
SOD	Superoxide dismutase
ss	Single strand
PC	Phosphocellulose
TEA	Triethylamine
TEAA	Triethylammonium acetate
TIC	Total ion chromatogram

General Introduction

Ribonuclease H

Ribonuclease H (RNase H) is an endoribonuclease, which hydrolyzes RNA strand of RNA/DNA hybrids, and produces 5'-phospate and 3'-hydroxy termini, and the activity of RNase H requires divalent metal ions, (Mg^{2+} and Mn^{2+}) [1]. RNases H are ubiquitous enzyme, found by all organism from bacteria to mammals [1][2][3][4], and RNase H was first detected in extraction of *calf thymus* by Hausen and Stein [1]. RNases H is classified into two types, type 1 and type 2 families which are based on the similarity of *Escherichia coli* (*E.coli*) RNase H. The type 1 enzymes are RNase HI, RNase H1 and retroviral RNase H, and type 2 enzymes are RNase HII, RNase HIII and RNase H2, which the difference of Roman or Arabic numerals are the difference of prokaryotes or eukaryotes [4][5]. The most of organisms, both of prokaryotes and eukaryotes, have multiple genes of RNases H, for example, *E.coli* has *rnhA* encoding RNase HI and *rnhB* encoding RNase HII [6][7].

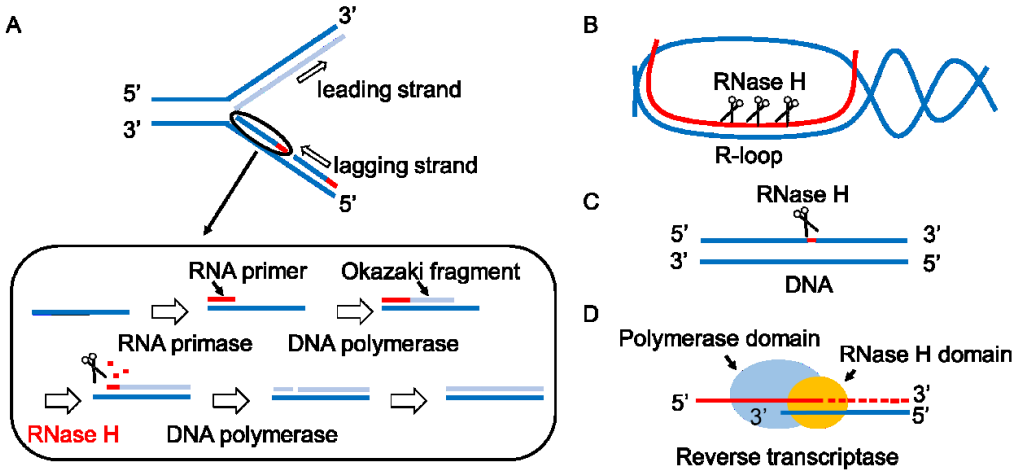

Fig. 1 The role of RNase H. (A) Primer of Okazaki fragment is cleaved. (B) Aberrant R-loop formation is removed and repair dsDNA. (C) Ribonucleotide monophosphates which are misincorporated into double strand DNA are removed. (D) Reverse transcriptase of retrovirus has RNase H domain which remove RNA chain from DNA.

Type 2 RNases H are the universal type, the most of organisms have the type 2 genes, and the similarities of amino acid sequences between type 1 and type 2 are quite different. The

difference of type 1 and 2 is not only the sequence, but also the enzymatic properties. RNases H has the important role of DNA replication and repairing and the main function of RNases H, both of type 1 and type 2, are the removal of RNA primers from Okazaki fragments [8][9], and type 1 RNases H resolves the R-loops which are the byproducts of transcription, and type 2 RNases H removes ribonucleotide monophosphates which are misincorporated into double strand DNA (Fig. 1) [10].

The enzymatic active sites of type 1 and type 2 RNases H are well preserved, and the active site is consisted by normally three aspartic acids and one glutamic acids, is called DEDD (Asp Glu Asp Asp) motif, and histidine residue is related to enzymatic activities of some RNases H [5]. The first crystal structures of *E.coli* RNase HI were reported by two laboratories at the same time in 1990 [11][12]. There are five α helices and also five β sheets, and the binding sites of divalent metal ions, which are the active site are located in α helices parts. The co-crystal structures of *E.coli* RNases HI with divalent metal ions have been solved, and the co-crystal structure with Mg^{2+} is a single metal ion, but on the other hand the structure with Mn^{2+} ions were two metal ions in the active site (Fig. 2) [12][13].

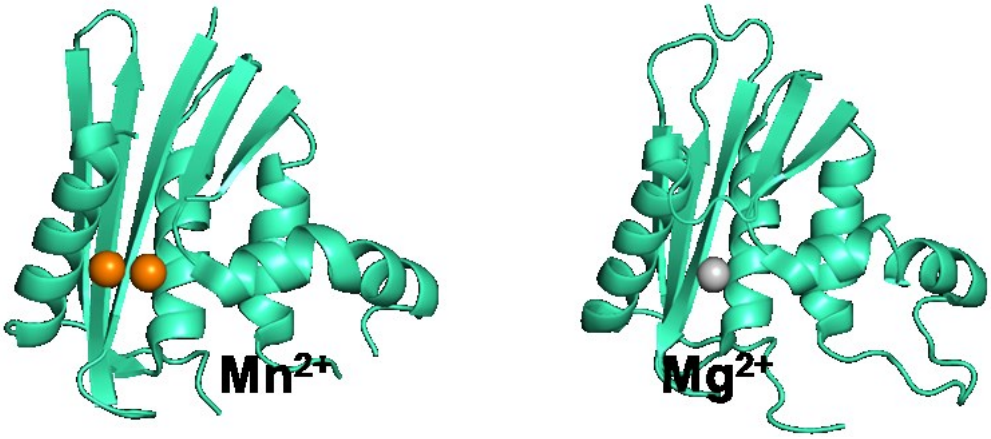

Fig. 2 Crystal structure of *E.coli* RNase HI from with metal ions (PDB ID: 1G15 (Mn^{2+}), 1RDD (Mg^{2+})

The RNase H domain of reverse transcriptase (RT) of human immunodeficiency virus type 1 (HIV-1) which is similar to *E.coli* RNase H (Fig. 3), had been studied and known that RNase H domain bound the two Mn^{2+} ions [14][15]. In addition, the activity of RNases H is decreased in high concentration of divalent metal ions, which led to the attenuation model [13]. The first

divalent metal ion gives the enzymatic activity and second divalent metal ion prevents the activity. These studies caused the possibilities that the mechanisms of RNase H activity is one or two metal ions catalysis [16][17]. The enzymatic activity of RNase H is the important to understand RT of HIV-1 and this leads to developing the inhibitors of RT.

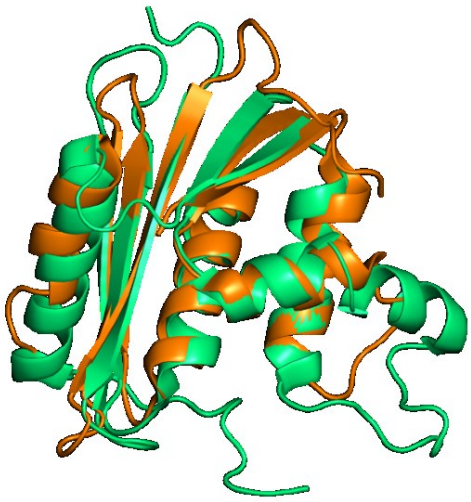

Fig. 3 The superimposition of crystal structures of RNase H domain of HIV-1 (orange) (PDB ID: 1HRH) and *Ecoli* RNase HI (green) (PDB ID: 1G15), and the RMSD is 3.302

In these days, various studies support that the mechanism of RNase H activity is two metal ions catalysis [18][19][20]. The mechanism of catalysis is shown in Fig. 4. The two metal ions are binding in DEDD motif, and one metal ion keeps the hydroxide ion in near phosphate ester bond, and also stabilize the transition state. The hydroxide ion attacks to phosphate as S_N2-like nucleophilic attack., and the anti-side oxygen of phosphate ester is displaced.

The first structure of the complex which is Bacillus halodurans RNase H and an RNA/DNA hybrid is reported in 2005 (Fig. 5 A) [21], and the crystal structure of Human RNase H1 with RNA/DNA hybrids were solved in 2007 (Fig. 5 B) [22]. RNases H has the binding domains of RNA and DNA, and the domains recognize the phosphate esters, sugars and bases of RNA and DNA, respectively [22][23]. These studies revealed the information of interaction to RNA/DNA hybrids and structures of RNase H active site. The crystal structures of the complexes of RNase H have been solved, but those RNase H were deactivated proteins which were mutated at the amino acid residues of the active site. Even if the analysis methods are improved, it will be difficult to detect the complexes with enzymatic activity.

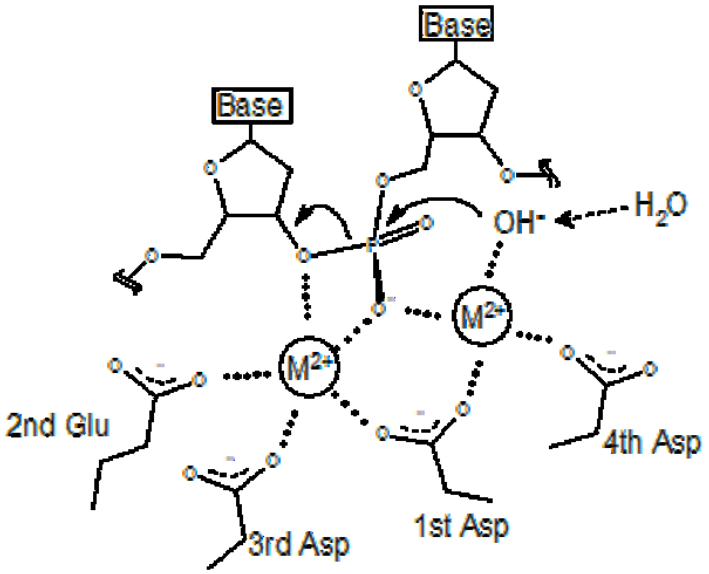

Fig. 4 The active site of RNase H, and DEDD motif.

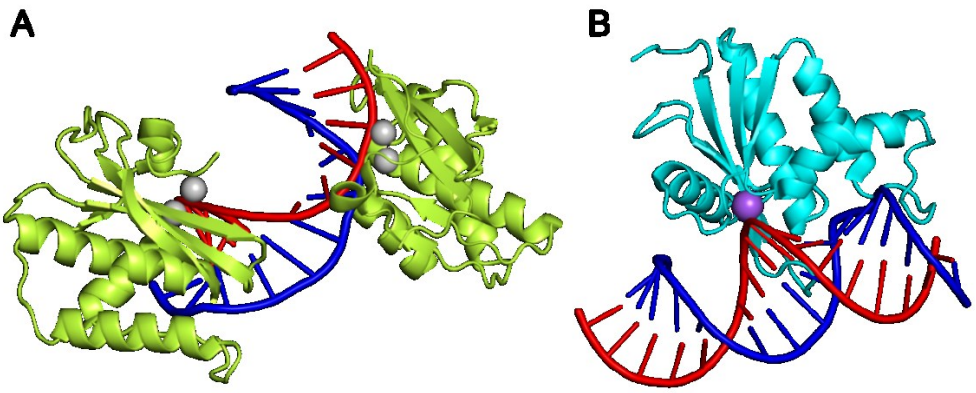

Fig. 5 (A) Co-crystal structure of *Bacillus halodurans* RNase H catalytic domain mutant D132N in complex with 12-mer RNA/DNA hybrid (red line: RNA, blue line:DNA) and Mg^{2+} ions (gray sphere) (PDB ID: 1ZBI), (B) Co-crystal structure of Human RNase H catalytic domain mutant D210N, RNA/DNA hybrid 18-mer and Na^{2+} ion (purple sphere) (PDB ID: 2QK9)

Analysis of Protein Structures by Native Mass Spectrometry

Proteins are composed of amino acid residues which arranged in specific sequence, and most of them fold the conformation. There are the four levels of protein structure which are called primary, secondary, tertiary, and quaternary structure. The primary structure is amino acid

sequence and modification, such as phosphorylation, glycosylation, and acylation etc. (Fig 6 A), and analyzed by Edman degradation and mass spectrometry (MS). The secondary structure is the shape of local segments of proteins, and the most ordinary secondary structures are α-helix and β-sheet, which are stable by hydrogen bonds (Fig 6 B). The tertiary structure is the three dimensional structure of a single chain protein (Fig 6 C). The quaternary structure is composed of multiple proteins, or proteins with metal ions, organic compounds, or others, and most of proteins are interacted with other molecules and get the functions (Fig 6 D). Secondary, tertiary and quaternary structures which are called higher order structure are analyzed by nuclear magnetic resonance (NMR), x-ray crystallography, and cryo-electron microscopy (EM) etc. [24][25][26], and those methods are improving year by year.

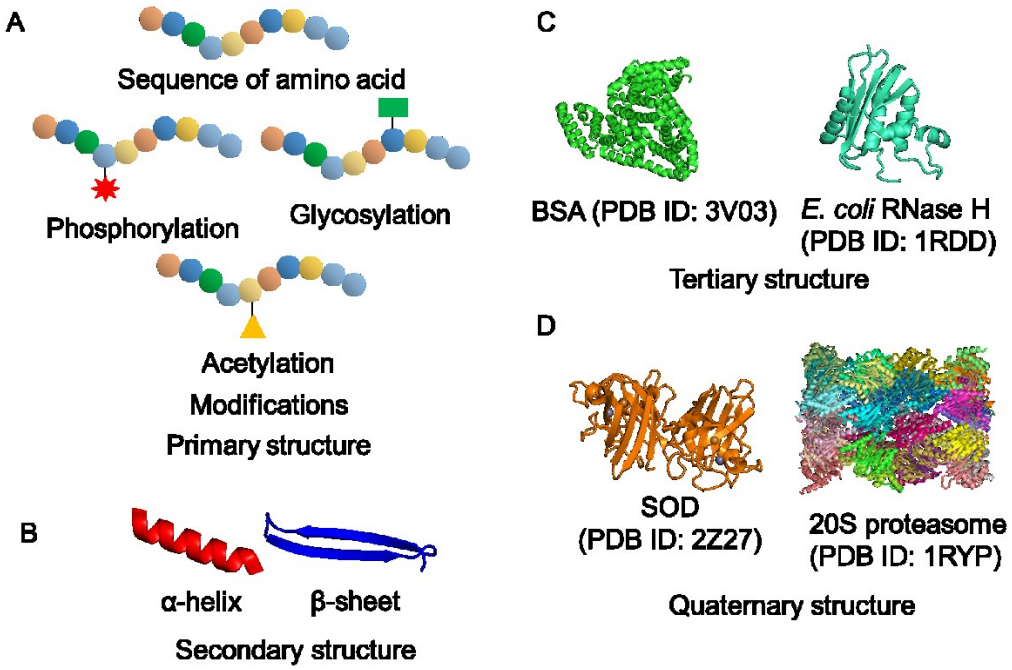

Fig. 6 The example of protein structures. (A) primary structure, (B)Secondary structure, (C)Tertiary structure, (D) Quaternary structure

It is important to reveal the protein structures and interactions, because it becomes not only to know the functions, but also to apply the development of medicines, or new high efficient catalysis etc. [27][28].

Nowadays, there are various powerful methods to detect structures in atomic level, but they are not always applied to analysis of proteins, because of the requirements of sample amount, crystal, purity, etc.: NMR requires a large quantity of sample, x-ray crystallography needs to makes crystals, and those methods are able to analyze only stable samples, when the unstable samples like enzyme-substrate complexes cannot be analyzed.

Recently, MS is used to analyze not only primary structure, but also higher order structure, ie. the stoichiometry of the complexes, and the analysis of proteins in native state is called "Native MS" [29]. Native MS cannot reveal the shape of proteins, but only the molecular masses and the number of charges, which reflects the number of charged amino acids and their locations. The method has some advantages, comparing with other methods: no need of the complicated preparation process, because native MS is based on electrospray ionization (ESI) -MS, thus we only prepare the proteins sample in volatile solution like ammonium acetate, or ammonium bicarbonate in near neutral pH, in addition, some studies show that sample solutions containing nonvolatile salts can be measured directly [30][31], this could make the optimal conditions of proteins in view of ion strength of solution or solubility. It requires small amount of sample (micromolar order) for one measurement. Native MS is becoming new method of analysis of protein complexes [32][33][34]. But native MS have some demerits like other methods, one of the demerits is that native MS has a little ability on quantitative analysis. Some studies show that size exclusion chromatography (SEC) could be connected to ESI-MS and detect the protein in native state, and permits both quantitative and qualitative analyses [35][36].

Study of This Thesis

In this thesis, I focus on the detection of RNase H and the complexes of RNase H, RNA/DNA hybrid and divalent metal ions (Mn^{2+}, Zn^{2+}) without mutation of protein using Native MS, and reveal the stoichiometry of the complex of RNase H with enzymatic activity. In addition, SEC-ESI-MS system is constructed for efficient analysis of proteins and protein complexes with a little amount of protein and short-time analysis, and detect the complex of RNase HI and human superoxide dismutase (SOD)-1 with Cu^{2+} and Zn^{2+} ions.

Chapter 1
Detection of the complex of native *E.coli* RNase HI

1-1. Introduction

E.coli has two genes of RNase H, *rnhA* of type 1 and *rnhB* of type 2, which encode RNase HI and RNase HII respectively [6][7]. *E.coli* RNase HI is composed of 155 amino acids and the molecular weight is 17600 [37] (Fig. 1-1), and secondary structures are consisted of five α-helix parts and five β-sheet part.

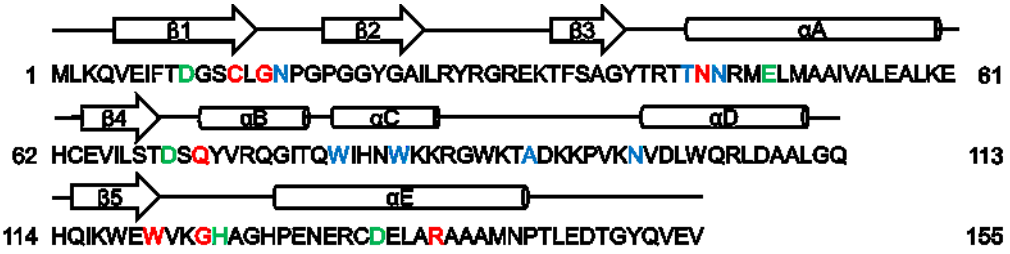

Fig. 1-1 The sequence and secondary structures of *Ecoli* RNase HI.

The crystal structures were solved in 1990, and the two independent laboratories reported at the same time [11][12]. The co-crystal structure of *E.coli* RNase HI with Mg^{2+} ion revealed the active site that single Mg^{2+} ion located around the acidic residues, which are D10, E48, D70 and D134 [13][14], On the other hand, the structure of RNase H domain of HIV-1 which is quite similar to the structure of *E.coli* RNase HI was revealed with Mn^{2+} ions (see General Introduction; Fig. 2), and there were two Mn^{2+} ions in the active site. In addition, the co-crystal structure of *E.coli* RNase HI with two Mn^{2+} ions was solved in 2001 [14]. *E.coli* RNase HI have been studied about the mutations of changing stability thermophilic, or deactivation [16][38][39][40][41]. The recognition of RNA/DNA hybrids was studied by crystal structure, and RNase HI had each binding site of RNA and DNA (Fig. 1-2).

Although the crystal structure of type 1 RNase H with RNA/DNA hybrids has been revealed [23], but the complex of non-mutated RNase H, RNA/DNA hybrid and divalent metal ions with enzymatic activity has not yet been detected, and the crystal structures of this ternary complex and that without the divalent ions have neither been solved.

In this study, I tried to apply the native MS to detect the ternary complex of the native *E.coli*

RNase HI, which retains the enzymatic activity. This is the first time to demonstrate that *E.coli* RNase HI, which has low affinity to Mn^{2+} ions without RNA/DNA hybrid, could gain the high affinity to two Mn^{2+} ions in presence of a RNA/DNA hybrid. It implied that the native MS allowed a snapshot of the transiently formed ternary complex of *E.coli* RNase HI, RNA/DNA hybrid, and Mn^{2+} ions.

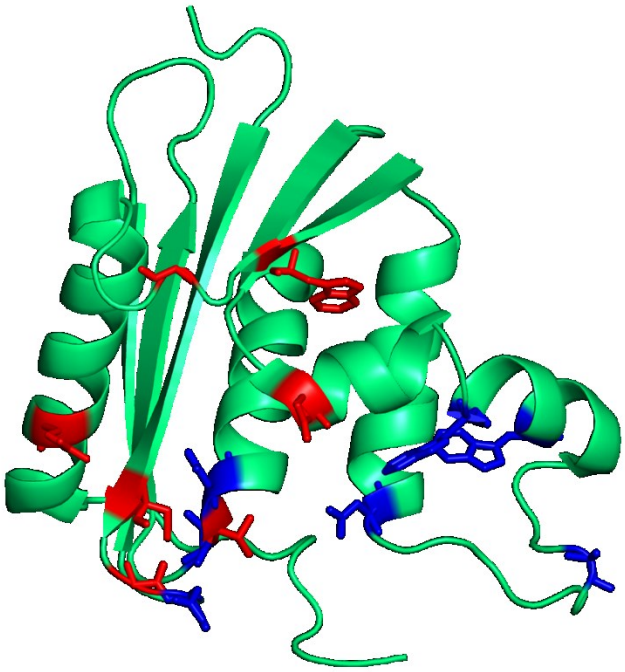

Fig. 1-2 The crystal structure of *E.coli* RNase HI and the binding site of RNA (red residues), and DNA (blue residues).

1-2. Materials and methods

Materials

The *rnhA* mutant *E.coli* strains MIC3009 [F, *supE44, supF58, lacY1 or* Δ*(lacIZY)6, trpR55, galK2, galT22, metB1, hsdR14(rK-,mK+), rnh-339:: cat*] [42] was kindly donated by Professor Shigenori Kanaya (Department of Material and Life Science, Graduate School of Engineering, Osaka University). ssRNA(8-mer; 5'-CGACACCU-3', 14-mer; 5'-CGACACCUGAUUCC-3') and ssDNA (8-mer; 5'-AGGTGTCG-3', 14-mer; 5'- GGAATCAGGTGTCG-3') were purchased

from Biologica co. (Aichi, JAPAN). RNase H (*E.coli*) was purchased from Takara Bio (Shiga, Japan). Ammonium acetate (NH_4OAc) MS grade was purchased from Fluka Analytical (Sigma-Aldrich, St. Luis, MO, USA), sodium chloride (NaCl), dithiothreitol and hydrochloric acid (HCl) were purchased from Wako (Tokyo, JAPAN), triethylamine, Sodium Lauryl Sulfate (SDS) and 0.2 mol/L-di-sodium dihydrogen ethylenediaminetetraacetate solution were purchased from nacalai tesque (Kyoto, JAPAN), Trifluoroacetic acid (TFA), Magnesium chloride hexahydrate 99.995%, acetic acid, Trizma base were purchased from Sigma-Aldrich (St. Luis, MO), SDS-PAGE gel, Prefect NT Gel (Buffer T-HCl, Gel conc. 5-20%, well 16W) was purchased from DRC (Tokyo, JAPAN), and SYPRO Ruby protein gel stain was purchased from Lonza (Rockland, ME, USA).Purified water was obtained using PURIC-ω highly pure water machine (ORGANO, Tokyo, Japan) in all experiments. Centrifugal vacuum concentrator was Rotary vacuum micro-concentrator RMC-24 (KOIKE PRECISION INSTRUMENTS, Osaka, Japan). AccuTOF (JMS-T100LC, JEOL, JAPAN) was used all MS measurement in this study. The analysis concentration of RNase HI, and the enzymatic activity, were used Series 1100 degasser, pump, column heater (HEWLETT PACKEARD, US) and DAD detector was 1260 Infinity (Agilent Technologies, Santa Clara, CA, US), and oligonucleotides purification was carried out by Automated Gradient controller (Waters, Milford, MA, US), degasser ERC-3415α (ERC, JAPAN), 515 HPLC pump (Waters, Milford, MA, US), UV detector Waters 2487 (Waters, Milford, MA, US), and Fraction collector FC204 (GILSON, Middleton, WI, US).

Methods

Expression and purification of RNase HI

E.coli MIC3009 was grown on streaked Luria-Bertani (LB) agar with ampicillin (50 μg/mL) plate at 32 ℃ for overnight. For the pre-cultivation, a single colony was picked up from the plate, inoculated into 2 mL liquid LB medium, and incubated at 32 ℃ for overnight. The pre-cultivated liquid was added into 1L liquid LB medium with ampicillin (50 μg/mL) and cultivated at 32 ℃. When the absorbance at 550 nm of the liquid was higher than 1.0, the temperature was raised at 42 ℃ for further induction, and cultivated for 4 hours [43]. Cells were harvested by centrifuging at 4000 rpm at 4 ℃ for 5 min; the supernatant was removed; the residue was added into about 20

mL 10 mM Tris-HCl (pH 7.4) buffer containing 100 mM NaCl, 1 mM EDTA, and 1 mM DTT (TE buffer 1), and suspended. The suspended solution was sonicated to lyse the cells. After the sonication, the solution was centrifuged at 4000 rpm for 15 min at 4 ℃. The phosphocellulose (PC) solution 4 mL (in TE buffer) was added into the supernatant and stirred by rotator at 4 ℃ for 2 hours. The solution with PC was applied to empty column, and PC was washed by 20 mL TE buffer 1 and eluted by 10 mL of 10 mM Tris-HCl (pH 7.4) buffer with 500 mM NaCl, 1mM EDTA and 1mM DTT. The fractions (500 µL each) were collected. Each fraction was checked by SDS-PAGE, and, for further purification, the fractions were concentrated by Amicon Ultra 0.5 mL tube (10 kDa cut), and the concentrated solution (50 µL) was applied to size exclusion chromatography (SEC), fractionated 1 min each, and checked by SDS-PAGE. The fractions were concentrated by Amicon Ultra 0.5 mL tube (10 kDa cut), and stored at -20 ℃. Before measurement, the stock solution was dialyzed against 10 mM NH_4OAc pH 7.0 by using an in-house dialysis system, and checked the concentration of RNase HI by HPLC. HPLC buffer A was 0.1 %TFA in H_2O, and B was 0.1 %TFA in ACN; the column was Intrada WP-RP 1.0 x 150 mm 3 µm (Imtact, Kyoto Japan); the flow rate was 80 µL/min, and the gradient was 5-40 min; 5-80%, 40-50 min; 80%, 51-51.1 min; 5%, 51.1-75 min; 5%.

The recombinant RNase HI, prepared in this study, was compared with a commercial product. Both preparations were purified by HPLC, and subjected to MALDI-MS (Fig. 1-3) and SDS-PADE (Fig. 1-4). Both analyses demonstrated the proteins to be pure.

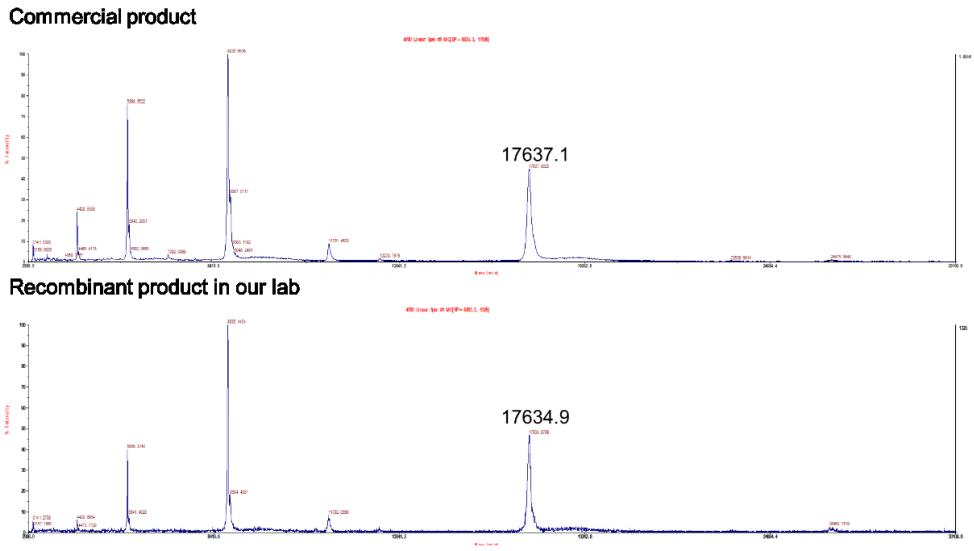

Fig. 1-3 MALDI-MS spectra of the commercial product and recombinant RNase HI.

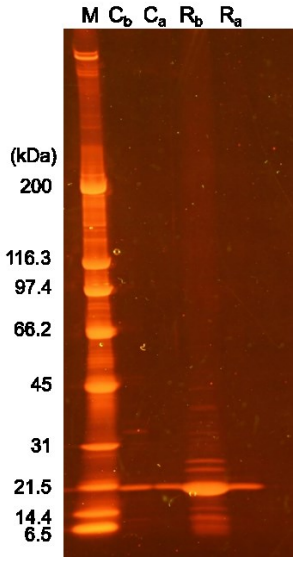

Fig. 1-4 SDS-PAGE of RNase HI. Commercial product before (C_b) and after (C_a) HPLC purification, and recombinant product before (R_b) and after (R_a) HPLC purification

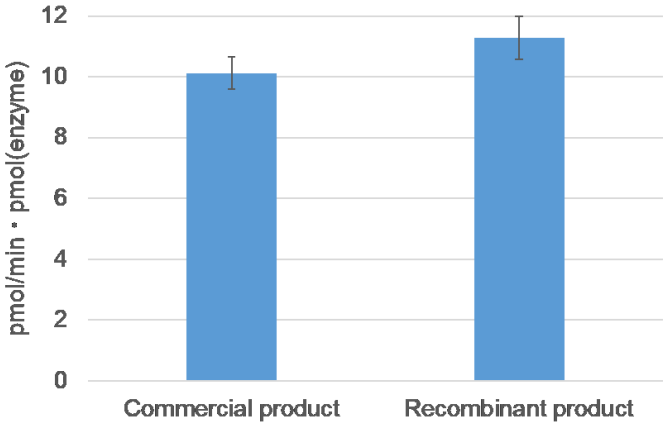

Fig. 1-5 Enzymatic activity of commercial and recombinant RNase HI.

In order to assess the enzyme activity of the above recombinant RNase HI, it was compared with the commercial one (Takarabio). First, both preparations were purified by reverse-phase HPLC. Then, the fractions were concentrated by centrifugal vacuum concentrator, and dialyzed against 10 mM Tris-HCl pH 7.4 containing 20 mM NaCl, 0.5 mM EDTA for 2 hours for refolding. Their enzyme activities were measured according to the method described below (Fig. 1-5). Note

that the less enzymatic activity of the commercial one could be attributed to the lower concentration (～10 μM) when handling or doing dialysis, causing sample loss by the adsorption to the surface of a tube or equipment. HPLC was performed on a column (Intrada WP-RP 1.0 x 150 mm 3 μm, Imtact, Kyoto) using a linear gradient: 5-40 min: 5-80%, 40-50 min: 80%, 51-51.1 min: 5%, 51.1-75 min: 5% of solvent B (0.1 %TFA in ACN) in solvent A (0.1 %TFA in H_2O) at flow rate of 80 μL/min. RNase HI (0.1 pmol/μL), RNA/DNA 8-mer (10 pmol/μL), and $MnCl_2$ (100 pmol/μL) were mixed and incubated for 5 min at 30 °C. Then, 0.1% TFA/water containing 1 mM EDTA was added for quenching, and subjected to HPLC.

Preparation of RNA/DNA hybrids

Single strand (ss) RNA, and ssDNA were dissolved in distilled water and adjusted to 1 nmol/μL respectively, and the solutions were stored at -20 ℃. Both of RNA and DNA were purified by HPLC, and removed the solvent by vacuum concentrator, and for completely removing TEAA, 100 μL 60% ACN 1% AcOH was added and removed the solvent by vacuum concentrator, and the wash steps were carried out twice time. HPLC buffer A was 0.1 M TEAA buffer pH 7.0, and B was 25% ACN in 0.075 M TEAA buffer pH 7.0, column was COSMOSIL 5C18-PAQ 4.6 x 150 mm, flow rate was 1 mL/min, injection volume was 40 μL (both ssRNA and ssDNA nmol/μL 5 μL was diluted to 40 μL) and the gradient was 0-40 min: 5-80%, 40-50.1 min; 80%, 50.1-60 min; 5%. The dried samples were dissolved in 10 mM NH_4OAc pH 7.0, and measured the 260 nm and decided the concentration. ssRNA solution and ssDNA solution were mixed equal mol.

Native MS

RNase HI solution was diluted with 60 %ACN, 1% AcOH (final conc.: 4 pmol/μL) for ordinary ESI-MS, and 10 mM NH_4OAc pH 6.0 for native MS, and those MS spectra were analyzed. All Samples were used Nanospray Tip (HUMANIX, Japan) for analysis. The all spectra were analyzed and fitted by ISOTOPICA (http://coco.protein.osaka-u.ac.jp/isotopica/)

Measurement of RNase HI under various concentration of $MnCl_2$

RNase HI and various concentrations of $MnCl_2$ were mixed and diluted with 10 mM NH_4OAc pH 6.0. The final concentration of RNase HI was 4 pmol/μL and $MnCl_2$ solution was 4, 8, 16, 40, 100, and 200 pmol/μL respectively. RNase HI solution was more than 200 pmol/ μ L, thus, the solution was diluted with 10 mM NH_4OAc pH 6.0 beforehand, normally it was adjust 100 pmol/μL. The pH of the solutions was checked to adjust 6 by pH test paper. The solutions were immediately measurement by MS.

Detection of the complex of RNase HI, RNA/DNA hybrids with/without Mn^{2+} ions

RNase HI (final conc. 4 pmol/μL), RNA/DNA hybrid 14-mer (final conc. 4, 8 pmol/μL) were mixed and diluted with 10 mM NH_4OAc pH 7.0 and immediately measured by MS.

RNase HI (final conc. 4 pmol/μL), RNA/DNA hybrid 14-mer (final conc. 4 pmol/μL) and $MnCl_2$ solution were mixed and diluted with 10 mM NH_4OAc pH 7.0, and immediately measured by MS (1.5 min after mixed ~). Because this condition was not able to detect the complexes, the condition which could detect the complexes was optimized, after optimization, the solution containing RNase HI (final conc. 4 pmol/μL), RNA/DNA hybrid 8-mer (final conc. 10 pmol/μL) and $MnCl_2$ (final conc. 0, 4, 8, 12, 16, 20 pmol/μL) solution were mixed and diluted with 10 mM NH4OAc pH 6.0, and measured by MS. RNA/DNA hybrids (10 pmol/μL) and various concentration of $MnCl_2$ (0, 4, 8, 12, 16, 20 pmol/μL) in 10 mM NH_4OAc pH 6.0 were analyzed.

Analysis of the complexes with other metal ions, Mg^{2+} and Ca^{2+} ions

RNase HI (final conc. 4 pmol/μL), RNA/DNA hybrid 8-mer (final conc. 10 pmol/μL) and $MgCl_2$ (final conc. 40, 80, and 200 pmol/μL) or $CaCl_2$ (final conc. 8, 16, 40 pmol/μL) solution were mixed and diluted with 10 mM NH_4OAc pH 6.0, and measured by MS.

Enzymatic activity

The Sample solutions were prepared same method as MS (8-mer, various conc. of $MnCl_2$), and the all solution volumes were 10 μL and incubated at 32 ℃ for 2 min, quenched with adding 10 μL 0.1% TFA 1 mM EDTA solution, and measured 260 nm peak by HPLC.

Buffer A was 0.1 M TEAA buffer pH 7.0, and B was 25% ACN in 0.075 M TEAA buffer pH 7.0, column was Cadenza CD-C18 1.0 x 150 mm 3 μm, flow rate was 80 μL/min, injection volume was 10 μL and the gradient was 0-5 min: 5-30%, 5-30 min; 30-60%, 30-31 min; 60-80%, 31-36.1 min; 80%, 36.1-50 min; 5%.

1-3. Results and discussion

Native MS

Fig. 1-6 shows MS spectra of RNase HI by ordinary ESI-MS and native MS, those spectra are obviously different of the charge state, the highest intensity of native MS is eight, and that of ordinary ESI-MS is sixteen, in addition, in ordinary ESI-MS, the charge states are wider range and native MS. The ordinary ESI-MS condition is easily to denature proteins including RNase HI, on the other hand, native MS condition is able to keep three dimensional structure of proteins, and the surface area of proteins in denatured state are larger than globular proteins including RNase HI in native state, and the binding sites of proton are increased, and ordinary ESI-MS condition which is contained AcOH can supply an abundance of protons, thus the spectrum of ordinary ESI-MS is detected higher charge state and wider range than native MS. In this way, the spectra can easily to discriminate the proteins whether in native state or in denatured state.

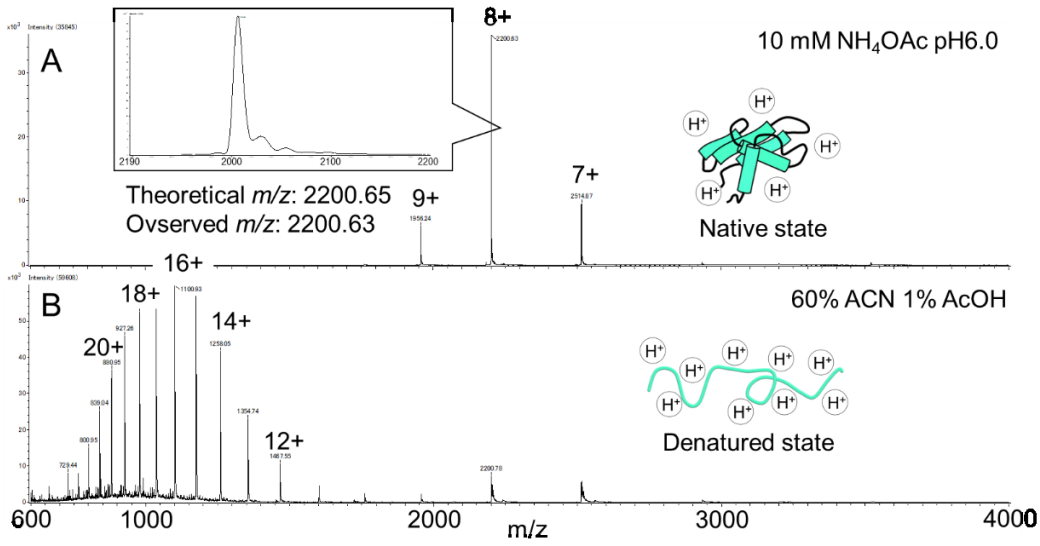

Fig. 1-6 The MS spectra of RNase HI in native MS(A), and general ESI-MS (B).

Measurement of RNase HI under various concentration of $MnCl_2$

RNase HI with various concentration of Mn^{2+} ions were detected (Fig. 1-7). The increase of the concentration of $MnCl_2$ increased the number of Mn^{2+} ions bound to RNase HI. This result is different from the crystal structure of RNase HI with two Mn^{2+} ions. If metal ions are specifically bound to proteins, the degree of metal ion adducts are not regularly increased in accordance with increase of the concentration of metal ion. The result did not suggest that Mn^{2+} ions were not bound to the active site of RNase HI in this condition. In addition, when protein solution with metal ions are measured by MS, metal ions normally bind to protein surface to be observed as the adduct ions. Thus, Mn^{2+} ions bound to RNase HI is unlikely to be incorporated into the active site of RNase HI, but to be on the surface of RNase HI. Mn^{2+} ions, which are reported to bind to the active site of RNase HI, could not detected clearly by native MS.

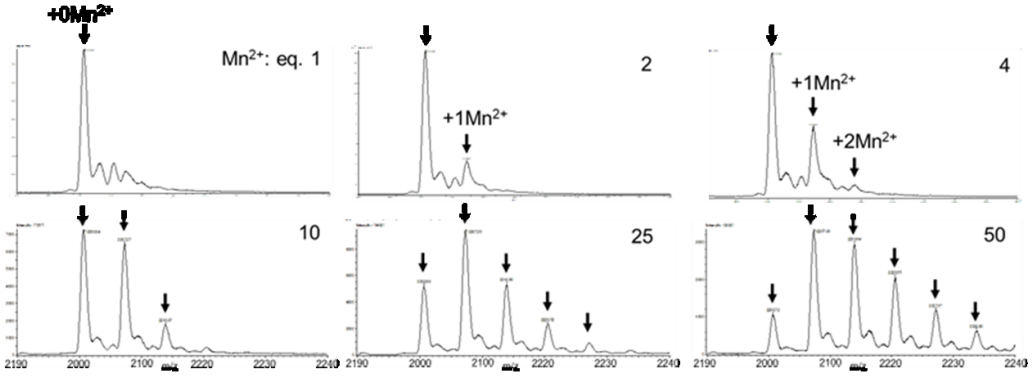

Fig. 1-7 The MS spectra of RNase HI (4 pmol/μL) with various concentrations of Mn^{2+} ion. The most left arrow indicates the peak of 8+ charged ion, and the right-handed arrows are the adduct ions of Mn^{2+} ions. The spectrum obtained in ammonium acetate buffer gave the adducts of 0 ~ 5 Mn^{2+} ions.

Measurement of a mixture of RNase HI and RNA/DNA hybrids

The complexes were easily detected for both RNA/DNA 8-mer (Fig. 1-8 A) and 14-mer (Fig. 1-8 B), and of course, all the spectra did not show any fragments of RNAs, because of the absence of divalent metal ion. When the concentration of RNase HI was increased, the peaks of 2:1 complexes started to be observed for both 8-mer (Fig. 1-8 C) and 14-mer (Fig. 1-8 D), but 14-mer was more easily to form the 2:1 complex than 8-mer. The crystal structure of the complexes of

RNase H from *B. halodurans* and human showed the 2:1 complex [22][23], which tended to be detected when the length of RNA/DNA hybrid was long, and dependent on the relative amounts of RNase HI. Thus, the results obtained by native MS were consistent with those of crystal structures. It should be noted that the spectrum of a mixture of RNase HI (8 pmol/μL) and RNA/DNA hybrid 8-mer (4 pmol/μL) did not show the intact peak, suggesting that the complex could be stable without divalent metal ion.

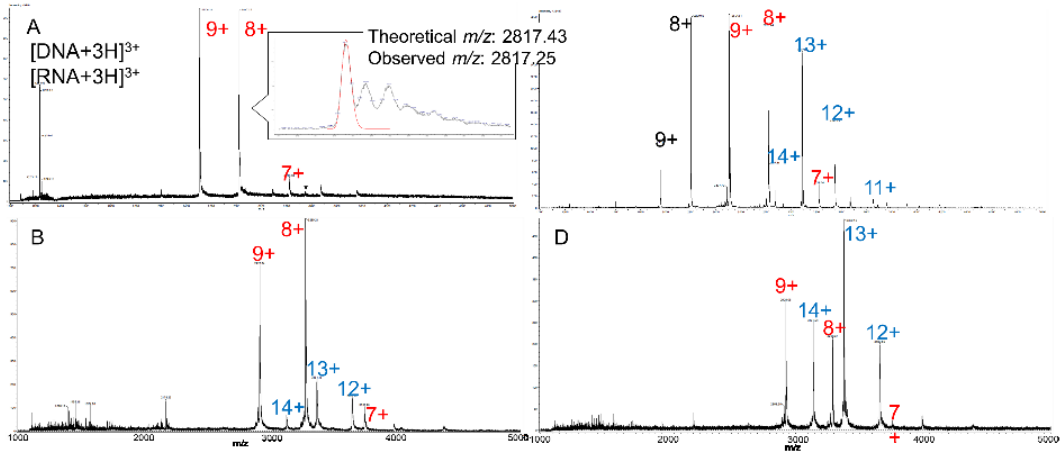

Fig. 1-8 The MS spectra of the complex of RNase HI and RNA/DNA hybrids. RNase HI (4 pmol/μL) and RNA/DNA hybrids 8-mer (A) and 14-mer (B) (4 pmol/μL) in 10 mM NH_4OAc pH7.0, and RNase HI (8 pmol/μL) and RNA/DNA hybrids8-mer (C) and 14-mer (D) in 10 mM NH_4OAc, pH7.0. The numbers on the peaks indicate the charge number: black number: RNase HI; red number: 1:1 complex of RNase HI and RNA/DNA hybrid; blue number: 2:1 complex.

Detection of the complex of RNase HI, RNA/DNA hybrids with Mn^{2+} ions

While the complex of RNase HI and RNA/DNA hybrid 14-mer was detected, the addition of Mn^{2+} ion into this solution did not give the ternary complex at all (Fig 1-9). Instead, the fragments of RNA and the complexes of RNase HI and ssDNA were detected, indicating that since the enzymatic activity was too fast to detect the ternary complexes with Mn^{2+} ions, RNA/DNA hybrid was hydrolyzed immediately. To detect the complexes with Mn^{2+} ions, it is necessary to keep the complexes without cleavage. The condition was optimized to detect the complexes by changing sample, salt concentration, pH, etc.

The ternary complex with Mn^{2+} ions could be obtained (Fig. 1-10 A), in which the conditions were as follows: RNase HI (4 pmol/μL), RNA/DNA hybrid 8-mer (10 pmol/μL) in 10 mM NH_4OAc, pH 6.0, Mn^{2+} ion (4-20 pmol/μL). The acidic pH decreased the activity properly, making it possible to detect the ternary complex. Mn^{2+} ions did not display the specific binding to RNase HI and RN/DNA hybrids (Fig. 1-11), but when RNase HI formed the complex with RNA/DNA hybrid, the binding affinity of Mn^{2+} ion was dramatically increased, and as the result, only 3 to 4 equimolar amounts of Mn^{2+} ion, two Mn^{2+} ions bound to form the ternary complex.

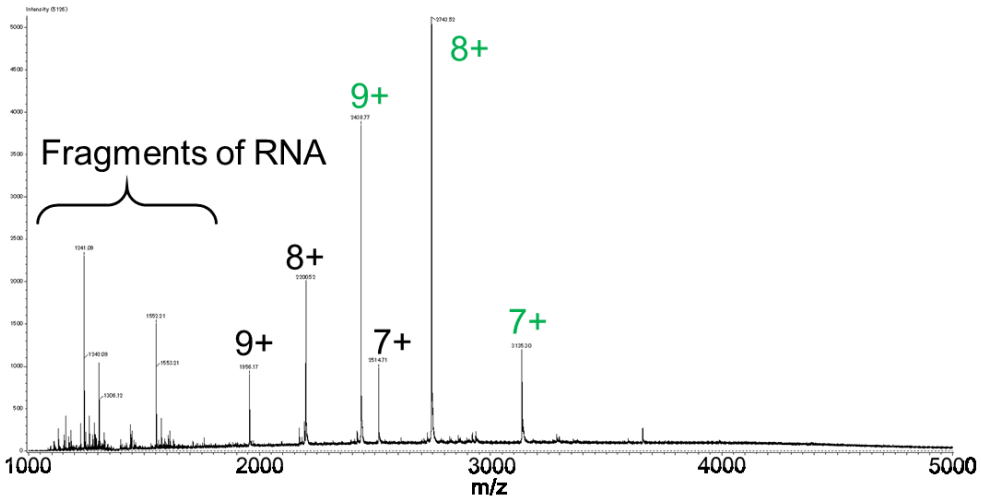

Fig. 1-9. MS spectrum of 10 mM NH_4OAc, pH 7.0 solution containing RNase HI (4 pmol/μL), RNA/DNA hybrid 14-mer (4 pmol/μL), and $MnCl_2$ (4 pmol/μL). The black numbers are RNase HI ion's peaks, and the green numbers indicate the complex of RNase HI and ssDNA (1:1).

RNA/DNA hybrid with Mn^{2+} ion solutions were examined, whether or not RNA/DNA hybrid had high affinity to Mn^{2+} ions. As the result, RNA/DNA hybrid did not display the high affinity to Mn^{2+} ions, the relative abundance of two Mn^{2+} ions bound to RNA/DNA hybrid was only 2.8%, while RNA/DNA hybrid occupied more than 70%. The result suggested that Mn^{2+} ion had the specific affinity to the complex of RNase HI and RNA/DNA.

Furthermore, the above reaction mixture stood for 4-5 min after mixing, then subjected to the same analysis as the above (Fig. 1-10 B). The complex of RNase HI, RNA/DNA hybrid, and two Mn^{2+} ions disappeared since the substrate, RNA/DNA hybrid, was almost hydrolyzed; the complexes of RNase HI with hydrolyzed RNA/DNA or ssDNA were newly detected. The

complex of RNase HI and intact RNA/DNA hybrid was slightly detected, which might owe to the lack of free Mn^{2+} ion in the reaction mixture by being trapped with fragmented RNA or ssDNA.

To analyze the time-dependent change of the complexes, the relative abundance of the ternary complex with 0, 1, 2 Mn^{2+} ions, which were obtained in the buffer containing $MnCl_2$, 16 pmol/μL, was integrated every 15 seconds from 1.5 to 3.5 min. The relative abundance of the complexes with one or two Mn^{2+} ions were calculated by ISOTOPICA (Fig. 1-12).

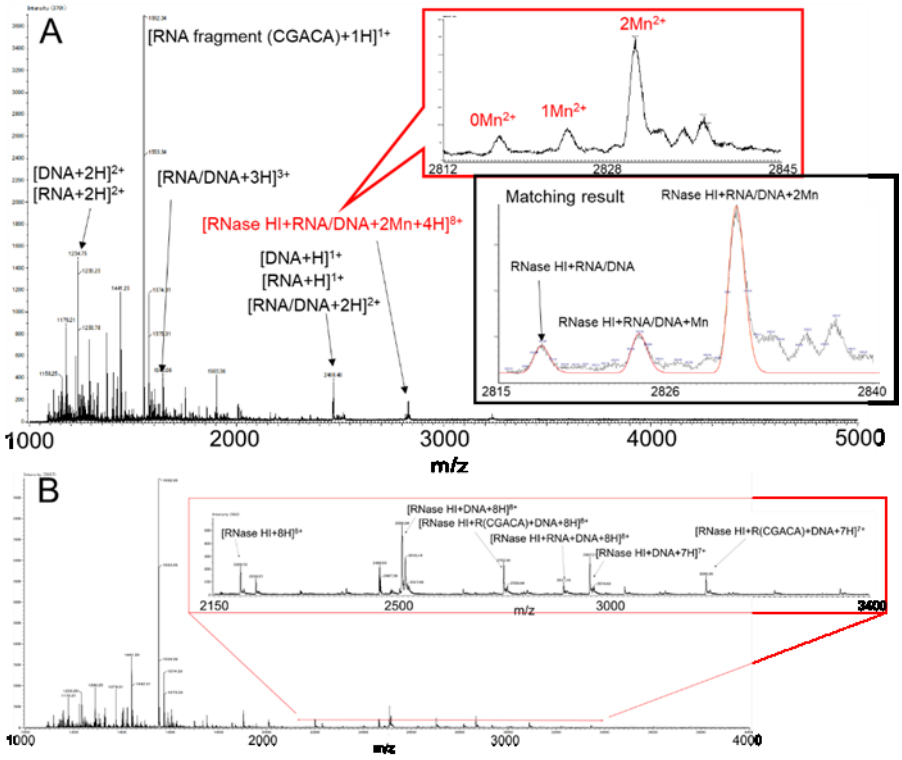

Fig. 1-10. MS spectrum of the ternary complex of RNase HI, RNA/DNA hybrid, and two Mn^{2+} ions in 1.5-2.5 min after mixing. The solution contains RNase HI (4 pmol/μL), RNA/DNA hybrid 8-mer (10 pmol/μL) and $MnCl_2$ (16 pmol/μL) in 10 mM NH_4OAc, pH 6.0. The inset shows the matching result by ISOTOPICA. $0Mn^{2+}$: $[RNase\ HI+RNA/DNA+8H]^{8+}$ at m/z 2187.49 (theo. 2817.43); $1Mn^{2+}$: $[RNase\ HI+RNA/DNA+Mn+6H]^{8+}$ at 2824.09 (theo. 2824.05); $2Mn^{2+}$: $[RNase\ HI+RNA/DNA+2Mn+4H]^{8+}$ at 2830.73 (theo. 2830.66) (A). MS spectrum of the ternary complex of RNase HI, RNA/DNA hybrid, and two Mn^{2+} ions in 4-5 min after mixing (B).

The measurements of native MS in this study takes 1.5 min in total to prepare the sample, mix it with $MnCl_2$ solution, load the solution to nanospray tip, and set to the ESI source. Therefore,

the time-dependent change of the complexes in Fig. 9 could be observed after 1.5 min.

The relative abundances of the complexes (0, 1, 2 Mn^{2+}) did not change until 2.25 min, but after 2.25 min, the complex with 2 Mn^{2+} ions decreased, in contrast, the complexes with 1 Mn^{2+} ion and without Mn^{2+} ion increased. The most of RNA/DNA hybrid was likely to be consumed by the hydrolysis with the enzyme, thereafter, the relative abundance of the complex with two Mn^{2+} ions decreased.

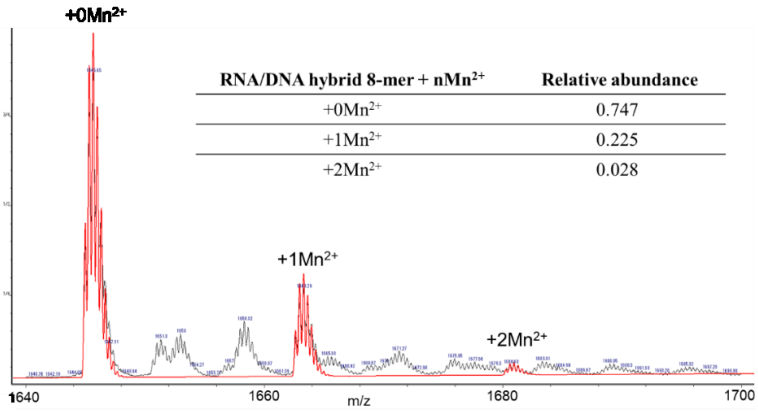

RNA/DNA hybrid 8-mer + nMn^{2+}	Relative abundance
+0Mn^{2+}	0.747
+1Mn^{2+}	0.225
+2Mn^{2+}	0.028

Fig. 1-11 Mass spectrum of a mixture of RNA/DNA hybrid 8-mer and Mn^{2+}ion. The solution contains RNA/DNA hybrid 8-mer (10 pmol/μL) and $MnCl_2$ (16 pmol/μL) in 10 mM NH_4OAc, pH 6.0. The red peak envelops are the theoretical ones calculated for each adduct of Mn^{2+} ions, which were fit to the actual spectrum by ISOTOPICA.

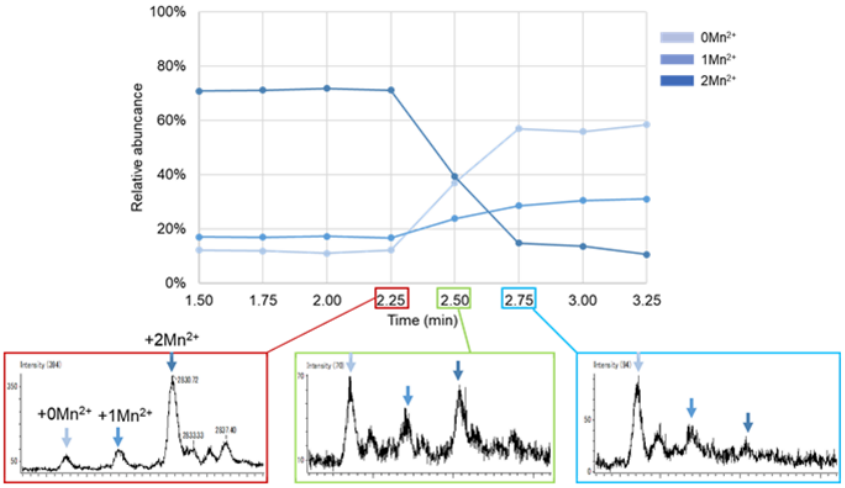

Fig. 1-12 The time-dependent change of the relative abundance of the complexes with 0, 1, 2 Mn^{2+} ions.

Analysis of the complexes with other metal ions, Mg^{2+} and Ca^{2+} ions

Mg^{2+} ion was also known as a cofactor of RNase HI. I tried to detect the complexes with Mg^{2+} ions similarly to the analysis of Mn^{2+} ion- complex. Along with the increase of Mg^{2+} up to 400 μM, the number of Mg^{2+} attached to the complex increased gradually (Fig. 1-13 B). The binding with Mg^{2+} ion was most likely to take place in a nonspecific manner. This might be because the dissociation constant (Kd) of RNase HI and Mg^{2+} ion was 0.71 mM, while that with Mn^{2+} was 0.035 mM. [44] From these evidence, Mg^{2+} ions have less affinity to the complex of RNase HI and RNA/DNA hybrid, comparing with the Mn^{2+} -complex (see Fig. 1-10), and behave as the adduct ions, despite that Mg^{2+} is essential for the enzymatic activity.

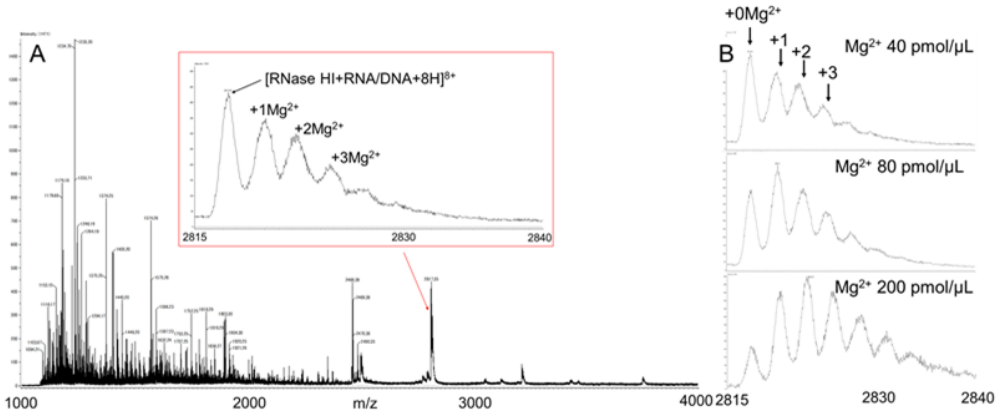

Fig.1-13 MS spectrum of RNase HI (4 pmol/μL), RNA/DNA 8-mer (10 pmol/μL), and $MgCl_2$ (40 pmol/μL) (A). Comparison of the MS spectra of this ternary complex under the various concentrations of Mg^{2+} ions (B).

Next, the binding of Ca^{2+} ion with the complex was examined, although Ca^{2+} ions did not have any effect on the enzymatic activity (Fig 1-14). When Ca^{2+} ions were added with ten equivalent to the complex, one or two Ca^{2+} ions were partially bound with the complex. The binding appeared to nonspecifically occur like Mg^{2+} case, and the number of Ca^{2+} attached was much less than that of Mg^{2+} -complex despite that Kd of Ca^{2+} (0.16 mM) [44] is less than Mg^{2+}.

The measurements of the complex under the presence of three kinds of divalent ions showed that the binding property of Mn^{2+} ion, observed in native MS, was different from others and RNase HI should have high-affinity binding sites to Mn^{2+} ions.

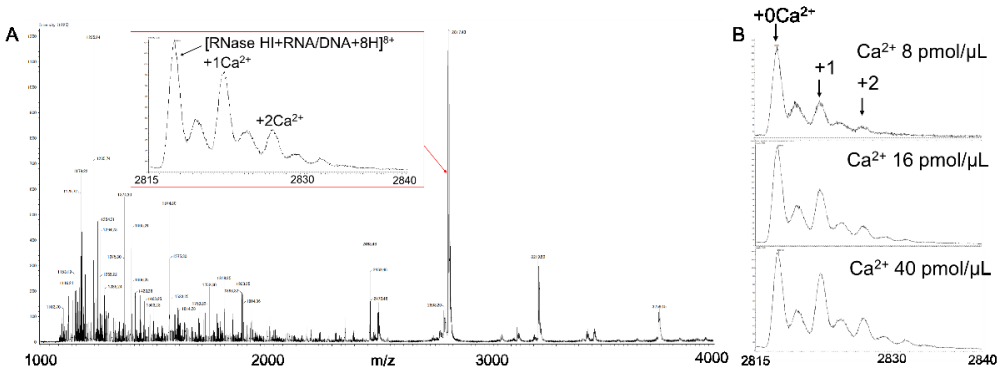

Fig. 1-14 MS spectrum of RNase HI (4 pmol/μL), RNA/DNA 8-mer (10 pmol/μL), and $CaCl_2$ (40 pmol/μL) (A). Comparison of the MS spectra of this ternary complex under the various concentrations of Ca^{2+} ions.

Enzymatic activity

The enzymatic activity and the relative abundance of the complexes with 0, 1, and 2 Mn^{2+} ions, observed by native MS, were shown in Fig. 1-15. The enzymatic activity increased as the abundance of two Mn^{2+} -complex becomes more (～74%) since it requires two Mn^{2+} ions for the activity. This result strongly suggested that two divalent metal ions were required for the enzymatic activity.

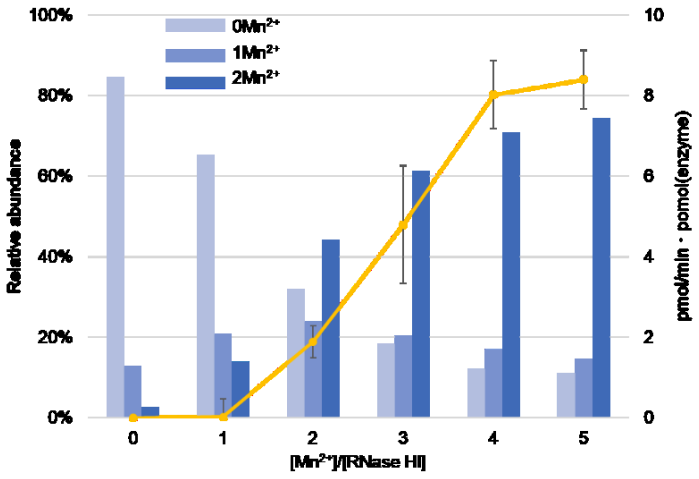

Fig. 1-15 The relationship between the enzymatic activity and the relative abundance of 0 to two Mn^{2+} ion-coordinated forms. The relative abundance of each form was calculated by ISOTOPICA. The spectra were integrated from 1.5 to 2 min.

1-4. Conclusion

The ternary complex of RNase HI, RNA/DNA hybrid, and Mn^{2+} ion, which has the enzymatic activity, could, for the first time, be detected by native MS. Although Mn^{2+} ion had low affinity to RNase HI in the absence of RNA/DNA hybrid, the ternary complex having two (not one) Mn^{2+} ions was transiently but specifically observed at 1.5 to 2 min after mixing these three components, which has the full enzymatic activity equivalent to the authentic enzyme.

Chapter 2
Characterization of RNase HI coordinated with Zn^{2+} ions

2-1. Introduction

As shown in the previous chapter, the complex of RNase HI, RNA/DNA hybrid, and two Mn^{2+} ions could be detected, which retains the enzymatic activity. Interestingly, the affinity of Mn^{2+} ions was dramatically increased, when RNase HI formed the complex with RNA/DNA hybrid. In addition, the relative abundance of Mn^{2+} ions in the complex was correlated with the enzymatic activity: when the relative abundance of the complex with two Mn^{2+} ions became the highest, the activity reached to the maximum (see Fig. 1-15).

RNases H coordinated with various kinds of divalent ions was well characterized. Some papers reported that Zn^{2+} ion affected the enzymatic activity: the RNase HI with Mn^{2+} or Mg^{2+} ions could hydrolyze the phosphorothioate RNA of RNA/DNA hybrid, but Zn^{2+} ion-form could hydrolyze the R-phosphorothioate RNA, but could not S- phosphorothioate RNA; Zn^{2+} ions with high concentration made HIV reverse transcriptase, which has RNase H domain, form a highly stable complex of enzyme-(primer-template), which inhibits the enzyme activity [45][46].

In this chapter, I described that Zn^{2+} ion could be specifically coordinated with RNase HI, and more preferably form the complex of RNase HI and RNA/DNA hybrid, which retains the higher enzymatic activity than that of the Mn^{2+}-form. It was also found that the enzyme retained the DNA chain after hydrolysis of the RNA chain and coordinated two Zn^{2+} ions. Furthermore, the enzyme with Zn^{2+} ions had a strong activity in the low concentration, but within a narrow range (1-2.5 μM). Taking into consideration the higher concentration of Zn^{2+} (0.2 mM) than Mn^{2+} (0.01-0.1 mM) or Mg^{2+} (10 mM) ions in a cell, Zn^{2+} ion might play an important role for the RNase HI's function.

2-2. Materials and methods

Materials

RNase HI and other reagents were described in chapter 2, and ZnCl2 99.999% was purchased from Sigma-Aldrich (St. Luis, MO, US)

Methods

Measurement of RNase HI under various concentrations of $ZnCl_2$

RNase HI and various concentrations of $ZnCl_2$ were mixed and diluted with 10 mM NH_4OAc pH 6.0, which was the optimized condition of $MnCl_2$.

The final concentration of RNase HI was 4 pmol/μL and the $ZnCl_2$ solution was 4, 8, 12, 80, 200, and 400 pmol/μL respectively. RNase HI solution was more than 200 pmol/μL, thus, the solution was diluted with 10 mM NH_4OAc pH 6.0 beforehand, normally it was adjusted 100 pmol/μL. The pH of the solutions was checked to adjust 6 by pH test paper. The solutions were immediately measurement by MS.

Detection of the complex of RNase HI, RNA/DNA hybrids and Zn^{2+} ions

RNase HI (final conc. 4 pmol/μL), RNA/DNA hybrid 8-mer (final conc. 10 pmol/μL) and $ZnCl_2$ (final conc. 0, 4, 8, 12, 16, 20 pmol/μL) solution were mixed and diluted with 10 mM NH_4OAc pH 6.0, and measured by MS. The solutions were immediately measured by MS, but it took 1.5 min for preparation after added $ZnCl_2$ solution.

To confirm the specific binding of Zn^{2+} ions, and Mn^{2+} ions, the complexes of Ca^{2+} ions which did not have the enzymatic activity were also measured in absence of and in presence of RNA/DNA hybrid 8-mer.

Enzymatic activity

The Sample solutions were prepared the same method as MS (8-mer, various conc. of $ZnCl_2$), and the all solution volumes were 10 μL and incubated at room temperature for 20 sec, quenched with adding 10 μL 0.1% TFA 1 mM EDTA solution and measured 260 nm peak by HPLC. The HPLC method was same as previous chapter.

2-3. Results and discussion

Measurement of RNase HI under various concentrations of $ZnCl_2$

Surprisingly, one Zn^{2+} ion was completely bound to RNase HI, with only two equimolar amount of Zn ion, and this singly Zn-adducted ion was kept up to the concentration of 12 μM of $ZnCl_2$ (Fig. 2-1), while Mn^{2+} ion was not bound specifically to RNase HI itself (Fig. 1-7) where the number of Mn^{2+} ions increased in proportion to the concentration of Mn^{2+} ion. Obviously, one Zn^{2+} ion was specifically bound to RNase HI, although the binding site of Zn^{2+} ions was not known by only this measurement. The second Zn^{2+} ion was not strongly bound to RNase HI. Increasing the concentration of Zn^{2+} ions, Zn^{2+} ions up to five equivalents to RNase HI were detected, which were the adduct ions.

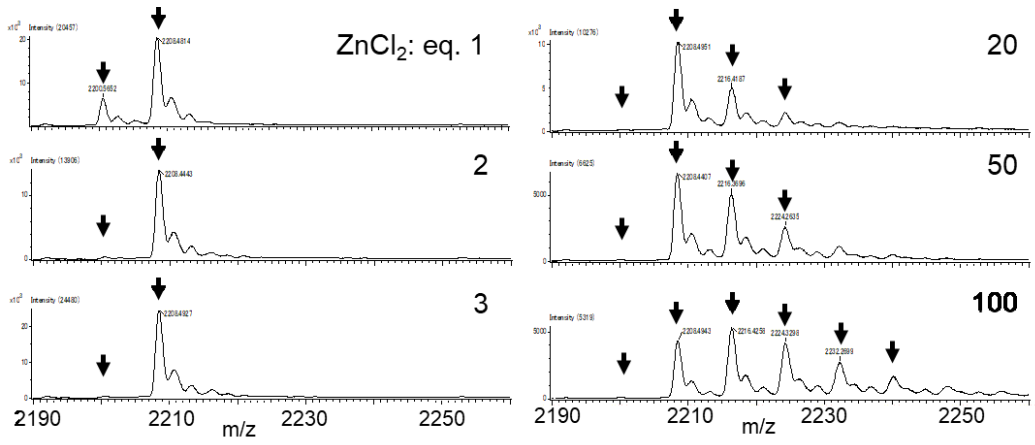

Fig. 2-1 The MS spectra of RNase HI (4 pmol/μL) in the presence of various concentrations of Zn^{2+} ion in 10 mM NH_4OAc, pH 6.0. The most left arrow is the peak of RNase HI (8+), the arrows next to which are the one, two, three, four, and five Zn^{2+} ions-adducted RNase HI.

Detection of the complex of RNase HI, RNA/DNA hybrids and Zn^{2+} ions

The complexes with Zn^{2+} ions were detected in the same way as that used for the detection of Mn^{2+} ions' complexes (Fig. 2-2), and to compare the difference of Mn^{2+} ions and Zn ions, Fig. 2-3 showed the MS spectra in the range of 4-5 min and 1.5-2.5 min after mixing, respectively.

In absence of RNA/DNA hybrids, one Zn^{2+} ion was specifically bound to RNase HI (Fig. 2-1), but in presence of RNA/DNA hybrids, the two Zn^{2+} ions were specifically bound to the

complex, which was quite similar to Mn^{2+} ion case, but the mass of the complex with two Zn^{2+} ion peak was matched with that calculated for the ternary complex, but plus 18 Da, which corresponds to H_2O. This result strongly suggested that the hydrolyzed RNA chains were resided in the enzyme. The bound H_2O was only detected for the ternary complex with two Zn^{2+} ions, while the ternary complex with one Zn^{2+} ion did not have H_2O (the inset of Fig. 2-2). The result implied that the second Zn^{2+} ion could initiate the hydrolysis of RNA chain.

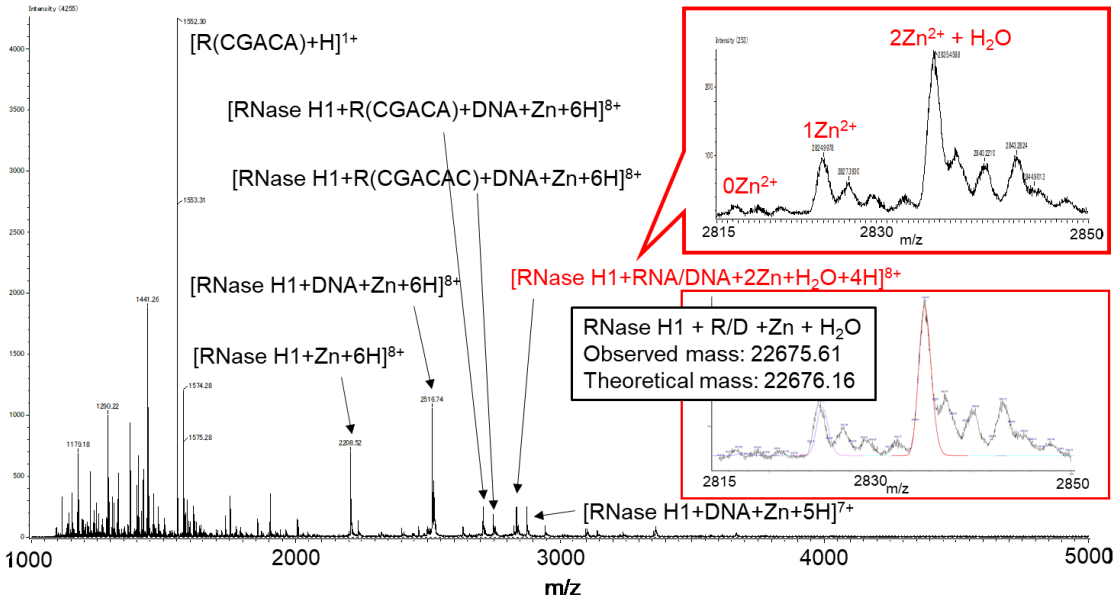

Fig. 2-2 The MS spectrum of 10 mM NH_4OAc, pH 6.0 solution containing RNase HI (4 pmol/μL), RNA/DNA hybrid 8-mer (10 pmol/μL), and $ZnCl_2$ (16 pmol/μL)

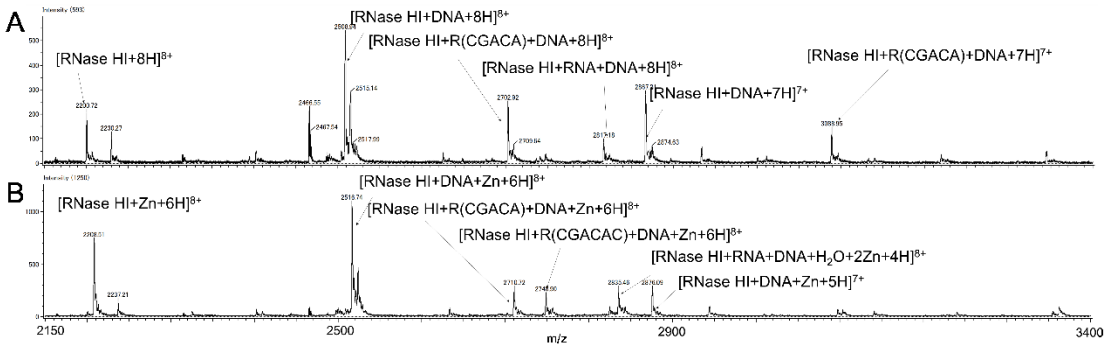

Fig. 2-3 MS spectra of RNase HI (4 pmol/μL), RNA/DNA hybrid 8-mer (10 pmol/μL), and $MnCl_2$ (16 pmol) (A); RNase HI (4 pmol/μL), RNA/DNA hybrid 8-mer (10 pmol/μL), and $ZnCl_2$ (16 pmol/μL) (B). The spectra were obtained in 4-5 min and 1.5-2.5 min, respectively, after mixing.

Next, in order to know the stability of the above unique complex of RNase HI, RNA/DNA hybrid, two Zn^{2+} ions, and H_2O, the reaction mixture was measured every 0.25 min between 1.5 and 3.5 min after mixing (Fig. 2-4). Interestingly, the relative abundances of the complexes with zero to two Zn^{2+} ions did not change; the complex with two Zn^{2+} ions was kept in this time range, although most of RNA/DNA hybrid was consumed; i.e. RNA chain was hydrolyzed. In addition, Katherine J. et al. [46] reported that Zn^{2+} ion stabilized the complex of HIV RT (RNase HI homologue) and primer-template (RNA/DNA hybrid), resulting in lowering the enzyme activity. The above result and the fact that higher concentration of Zn^{2+} attenuated the activity (see Fig. 2-6) are quite similar to the HIV RT case.

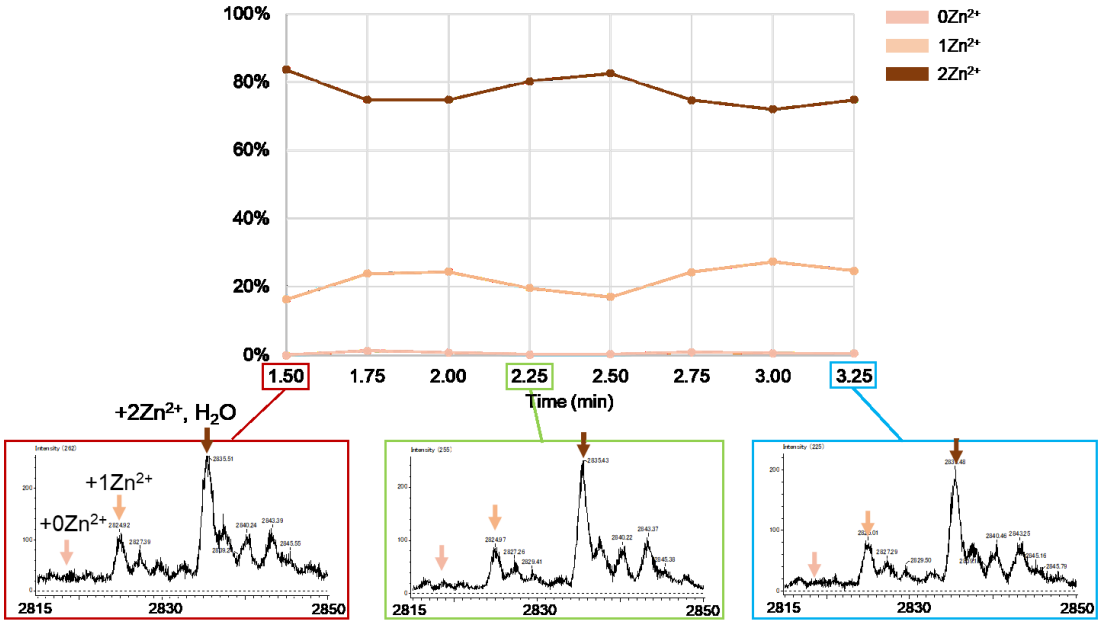

Fig. 2-4 The relative abundance of the complexes with 0, 1, 2 Zn^{2+} ions. The complex with two Zn^{2+} ions corresponds to that with one H_2O.

Enzymatic activity

Fig. 2-5 showed the relative abundance of 0, 1, 2 Zn^{2+} ion –complexes, observed in native MS, with the plot of the activity at each time point. The activity measured at each time point did

not match with the relative abundance of the two Zn^{2+} ion –complex, which was thought to the active form, unlike the case of Mn^{2+} -complex (Fig. 1-15). In addition, the relative ratios of the complexes with 0, 1, and 2 Zn^{2+} ions were not changed with three to five equivalent of Zn^{2+} ion, and two Zn^{2+} -complex turned out to be the ternary complex but with the hydrolyzed RNA. Note that the ternary complex with one Zn^{2+} hold the intact RNA/DNA hybrid and one Zn^{2+} ion could associate specifically with RNase HI (see Fig. 2-2). From the line of evidence, the ternary complex with one and two Zn^{2+} ion, obtained with over three equivalent of Zn^{2+} ion in Fig. 2-5, should be the end products that could not turn over or shift to other complexes. Although the location of two Zn^{2+} ions in the complex needs to be clear, the location of Zn^{2+} ion in the singly Zn^{2+} -complex, observed with over three equivalent Zn^{2+} ion, might not be the active form, but resided in other specific site of RNase HI to stabilize the complex with the RNA/DNA hybrid.

The activity of Zn^{2+} -complex was relatively higher than Mn^{2+} -complex, although the condition of reaction was not exactly the same. In case of Zn^{2+}, the incubation time was much shorter (20 sec) because the longer incubation time (2 min) used for the case of Mn^{2+} could not give the products during degradation process; i.e. the enzymatic reaction of the Zn^{2+} -complex was too fast to detect on-going products with various concentrations of Zn^{2+} ion. RNA/DNA hybrids were degraded within 2 min with 16 μM Zn^{2+} even at lower temperature, 22 ℃ (32 ℃ was used for Mn^{2+} -complex).

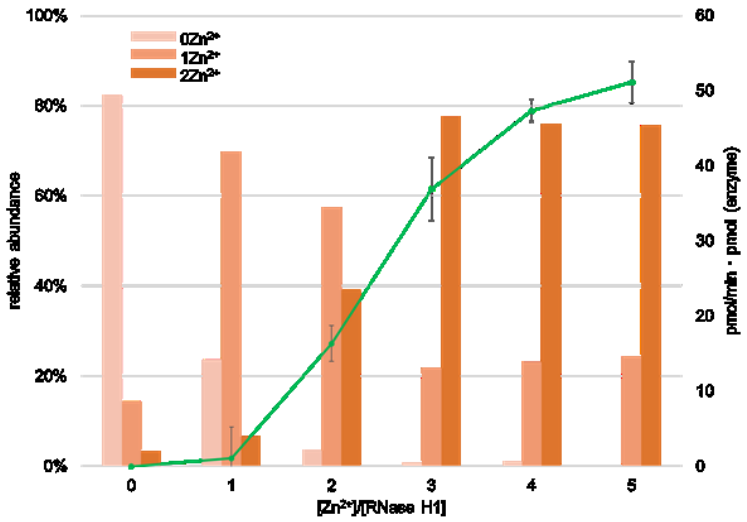

Fig. 2-5 The relationship between the enzymatic activity and the relative abundance of 0 to two Zn^{2+} ion-coordinated forms. The relative abundance of each form was calculated by ISOTOPICA. The spectra were integrated from 1.5 to 2.5 min.

To make the functional difference between Mn^{2+} and Zn^{2+} -complexes clear, the activities of both forms were measured under the same conditions (Fig. 2-6). The highest activity of Zn^{2+} -form was higher than Mn^{2+} -form, but the high activity of Zn^{2+} -form was kept in limited range of Zn^{2+} ions, and significantly reduced with over 50 equivalent mol concentration. The highest activity of Zn^{2+} -form was obtained with ten mol-equivalent concentration of Zn^{2+} ion and 1.18 times higher than that of Mn^{2+} -form.

It has not been reported that Zn^{2+} ion afforded the high activity to RNase H with relatively low concentration. In turn, the higher concentration of Zn^{2+} ion rendered RNase HI to be less active. This evidence shall be further studied.

Wang, D., et al. [47] reported that the total concentration of Zn^{2+} ion in *E.coli* was ~0.2 mM; the free Zn^{2+} ion was about 20 pM. Moreover, although the concentration of RNase HI in *E.coli* has not been measured, the concentrations of proteins in cell are normally nM ~ μM order. Since RNase HI has strong affinity to Zn^{2+} ion even in absence of RNA/DNA hybrids, it could associate with Zn^{2+} ion in the cell with more likelihood than other divalent ions (Mn^{2+}, Mg^{2+}), which might be involved with the endogenous enzymatic activity.

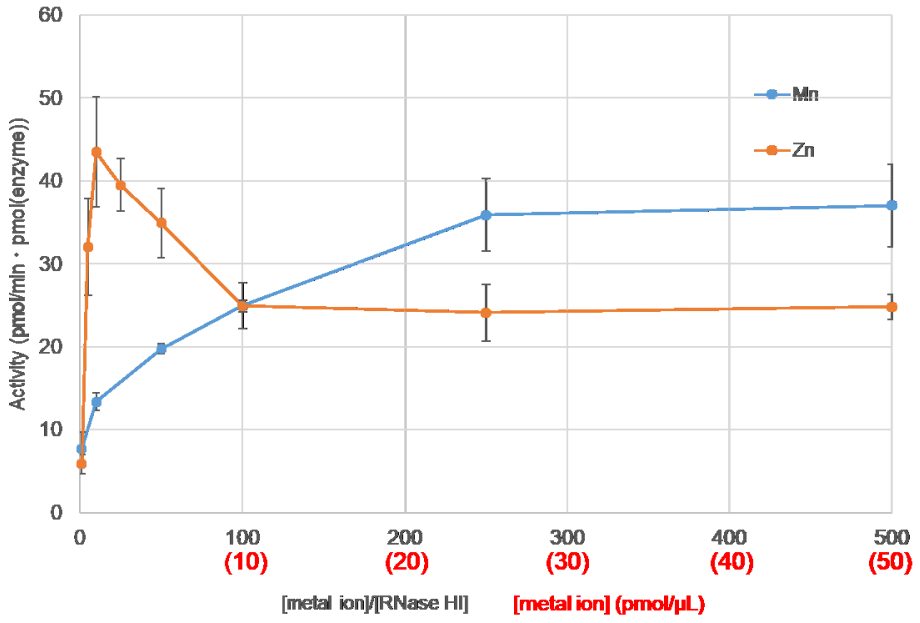

Fig. 2-6 The plots of the enzymatic activities of Mn^{2+} and Zn^{2+} -complexes as function of molar equivalents of each divalent ion.

2-4. Conclusion

Zn^{2+} ion had a strong affinity to RNase HI in absence of RNA/DNA hybrids, which was not observed in the case of Mn^{2+}, and only one Zn^{2+} ion was associated with RNase HI, implying that RNase HI should have a specific Zn^{2+} binding site. It is interesting to speculate that nascent RNase HI after being expressed in a cell has already been associated with one Zn^{2+} ion, and then, with the second divalent ion such as Zn^{2+}, Mn^{2+}, or Mg^{2+} together with a substrate to hydrolyze the RNA chain.

The ternary complex with Zn^{2+} ion could be formed with the stoichiometry of RNase HI: RNA/DNA hybrid: Zn^{2+} = 1: 1: 2, which was the same as Mn^{2+} case. However, it is noteworthy that two Zn^{2+} -complex, observed in MS, was the ternary complex but with the hydrolyzed RNA. Since the reaction rate of Zn^{2+} -form was faster than Mn^{2+} -form (Fig. 2-6), the active ternary complex before the reaction has not ever been observed. Nevertheless, it strongly supports that RNase HI functions with the two metal ions' catalysis.

Although the enzymatic activity was attenuated with higher concentration of Zn^{2+} ion (50 μM～), RNase HI exhibited 1.18-times higher activity than Mn^{2+} -complex, and moreover, at low concentration (1 μM) of Zn^{2+} ion, the activity increased 3.25-times high in comparison with that of Mn^{2+} -complex (Fig. 2-6). Zn^{2+} ion might raise the stability of RNase HI itself or the complex, which was partly supported by observation of the ternary complex that retained the hydrolyzed RNA chain, which was released for the case of Mn^{2+} -complex.

These results suggest the new catalytic mechanism of RNase HI that needs to be elucidated by further studies with calorimetric, X-ray analyses, etc.

Chapter 3
Analysis of protein complexes using Size exclusion chromatography-electrospray ionization mass spectrometry

3-1. Introduction

In previous chapters, the result showed the usability of native MS to analyze the protein complexes. Although native MS is the powerful method for the component analysis of the complex, native MS is not suitable for quantitative analysis. In order to compensate the drawback of the native MS, high-speed size-exclusion chromatography (SEC), which allows the separation and quantification of complexes based on UV absorption, was connected to ESI-MS.

SEC is a separation method based on sizes and shapes of molecules in solutions. The resin has a fixed pore through which sample molecules are permeated, i.e. those smaller than the pore size enter into the inner part of the resin, while those bigger ones do not, which makes them to separate with different retention times (Fig. 3-1).

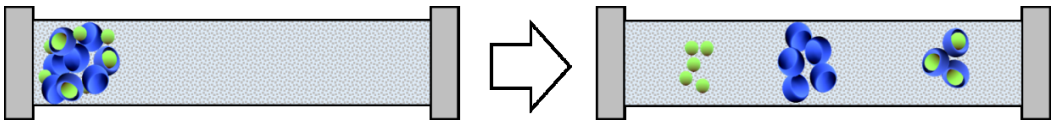

Fig. 3-1 The separation in SEC, the elution time of large molecules is faster than small molecules.

The detection of SEC is generally used UV detector. UV detector is useful way to detect proteins because proteins have UV absorption around 210 nm (peptide bonds) and 280 nm (aromatic compounds), but UV can only detect the molecules and obtains the intensity of the peak. Recently, SEC connected with ESI-MS system to analyze proteins was reported, and this system allowed not only for the qualitative and quantitative analysis, but also for proteins or protein complexes being analyzed in native states [48][49][50]. Note that MS has the capability to reveal the components of a complex such as a ligand, metal ions, proteins, etc. in various measurement modes such as MS/MS, which is useful for determining the stoichiometry of the components of a complex (Fig. 3-2).

When we want to get the information of complexes with small molecules, UV detector is not useful way except small molecules having specific UV absorption, but MS can detect not only small molecules, but also the number of them which are bound to protein. Moreover, the relative

abundance of the complexes, the small molecules, or metal ions with proteins can be easy to analyze.

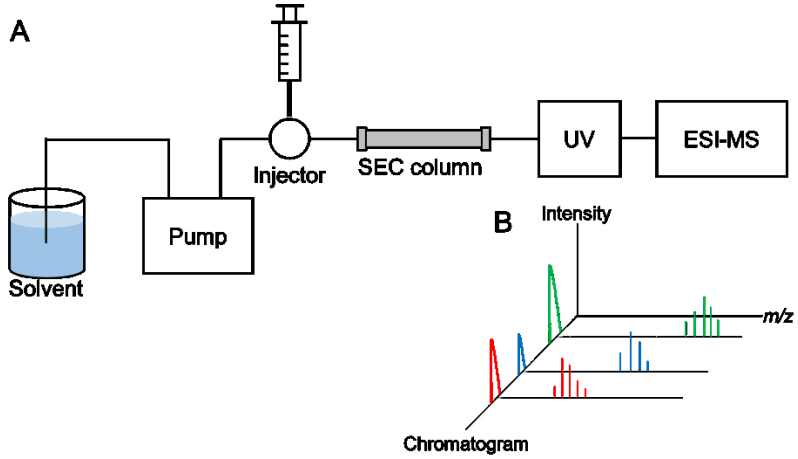

Fig. 3-2 (A) The components of SEC-ESI-MS and (B) the three dimensional chromatogram which was obtained from SEC-ESI-MS.

In this chapter, SEC was combined with native ESI-MS, and detect protein and protein complexes in native state. The general SEC system needed too many protein samples to analyze, thus, the SEC column was optimized for protein analysis. A small amount protein analysis is one of the most important things to understand the functions or structures.

This chapter showed the result of the qualitative and quantitative analysis, and the complex of RNase HI and RNA/DNA hybrid, and synthesized human superoxide dismutase which formed homodimer with metal ions analyzed by SEC-ESI-MS.

3-2. Materials and methods

Materials

The reagents were used as same as previous chapters. Myoglobin from *Equus caballus* was purchased from, bovine Super oxide dismutase (SOD) -1 was purchased from MP Biomedicals (Solon, OH, US), ovalbumin was purchased from Sigma-Aldrich (St. Luis, MO), human SOD-1 was donated by Mr. Toshiki Takei (Institute for protein research, Osaka university). SEC column was Agilent Bio-SEC-3 100 Å repacked in metal free column PEEK column 2.1 x 250 mm (GL science, Tokyo, Japan), pump was Ultimate Swichos pump (Dionex, Germany). Bio-inert pump

was 1260 Infinity II Bio-Inert Pump (Agilent Technologies, Santa Clara, CA, US). Spray was AccuTOF spray replaced inner stainless capillary with fused-silica capillary.

Methods

Qualification and Quantification

To check the performance of the SEC-ESI-MS system, whether proteins in native state could be detected or not, myoglobin which had heme (100 pmol), and SOD-1, homodimer including Cu and Zn ion (dimer 50 pmol), were measured by SEC-ESI-MS respectively. To compare with native MS, myoglobin (4 pmol/μL) and SOD-1 (dimer 10 pmol/μL) were measured. All measurement in this study, the injection volume was 1 μL, and the elution buffer was 100 mM NH_4OAc pH 7.0, 5% ACN, flow rate was 80 μL/min, and UV detection was 214 nm. The electrospray was carried out by using a normal ESI spray needle which has a coaxial double layered pipes with 100 μm diameter, the outer of which was used for nebulizing gas (nitrogen), which was important for making a homogeneous fine droplets. Note that the use of ACN as an additive (5%) was for improving the stability of the spray, which did not perturb protein structures as a complex. The protein mixture, OVA (45 kDa), SOD-1 (dimer 32 kDa), myoglobin (18 kDa), 50 pmol/μL respectively, was measured, and compared UV spectrum and ion chromatogram. For quantification analysis, various concentrations of myoglobin (injection amounts: 25, 50, 100, 200 pmol) were analyzed and the peak areas were calculated by MassCenter (JEOL, Tokyo, JAPAN).

Analysis of the complex of RNase HI and RNA/DNA hybrid.

To check the elution time, RNase HI (injection volume; 50 pmol) and RNA/DNA hybrid 14-mer with 100 mM EDTA were measured. The mixture solution of RNase HI and RNA/DNA hybrid 14-mer (injection volume: 50 pmol each) in 100 mM NH_4OAc pH 7.0, 5% ACN without 10 mM EDTA solution and RNase HI and RNA/DNA hybrid 14-mer (injection volume: 50 and 25 pmol) in 100 mM NH_4OAc pH 7.0, 5% ACN with 10 mM EDTA solution were measured.

Analysis of human SOD-1

Human SOD-1 with and without the metal ions (Zn^{2+} ion and Cu^{2+} ion) was measured by SEC-ESI-MS [51]. The injection volume was 1 μL, and the elution buffer was 100 mM NH_4OAc pH 7.0, 5% ACN, and UV detection was 214 nm.

3-3. Results and discussion

Qualification and Quantification

Myoglobin is the one of the hemeprotein, and the affinity of apo-protein for heme has quite large dissociation constants (10^{-12} ~ 10^{-15} M) [52], thus the holo-myoglobin is easy to detect in native MS. When myoglobin was measured in 60% ACN, 1% AcOH solution, myoglobin was detected as an apo form (Fig. 3-3).

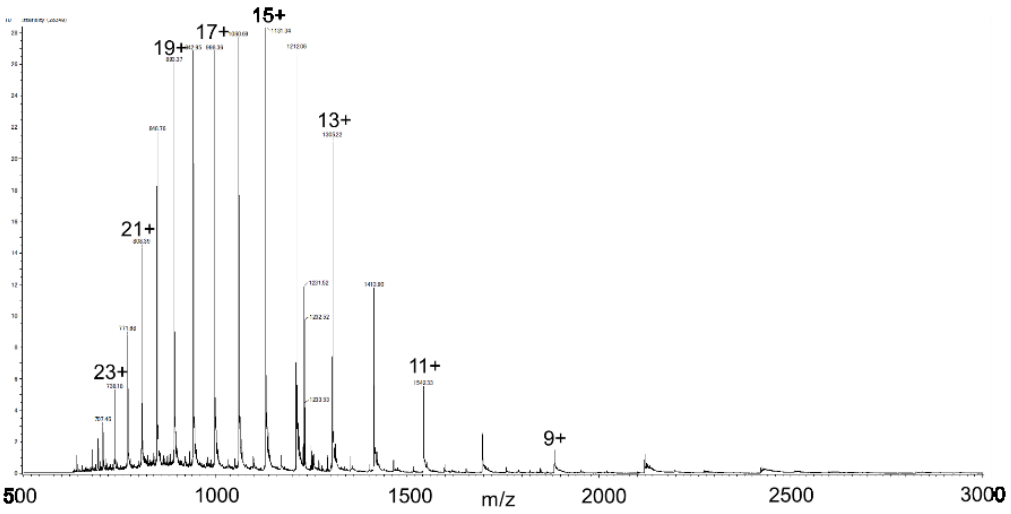

Fig. 3-3 The MS spectrum of myoglobin in 60% ACN and 1% AcOH solution measured by nanoESI-MS. The number showed the number of charges, and all the peaks were assigned to the apo-form (MW = 16951.60952).

The SEC-ESI-MS of myoglobin was shown in Fig. 3-4. Holo-myoglobin could be detected with heme. In addition, bSOD-1, which is a homodimer coordinated with Zn^{2+} and Cu^{2+} ions, was measured by SEC-ESI-MS, SOD-1 could also be detected as a homodimer (Fig. 3-5). SEC-ESI-

MS system could detect the protein complexes with small compounds such as a heme or metal ions.

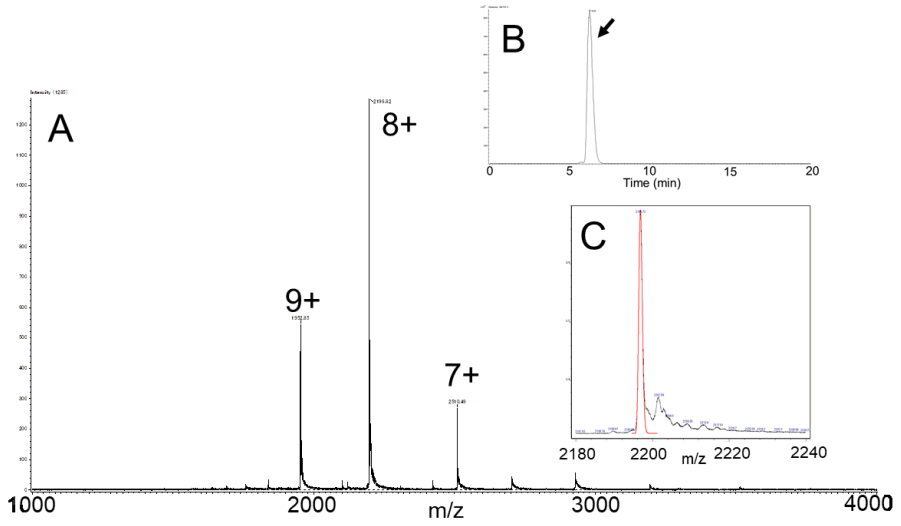

Fig. 3-4 (A) The MS spectrum of myoglobin measured by SEC-ESI-MS, and (B) TIC. (C) Fitting peak (8+) of theoretical m/z (2197.02; red line) and observed m/z (2196.86; black line), and the peaks were detected as holo-form.

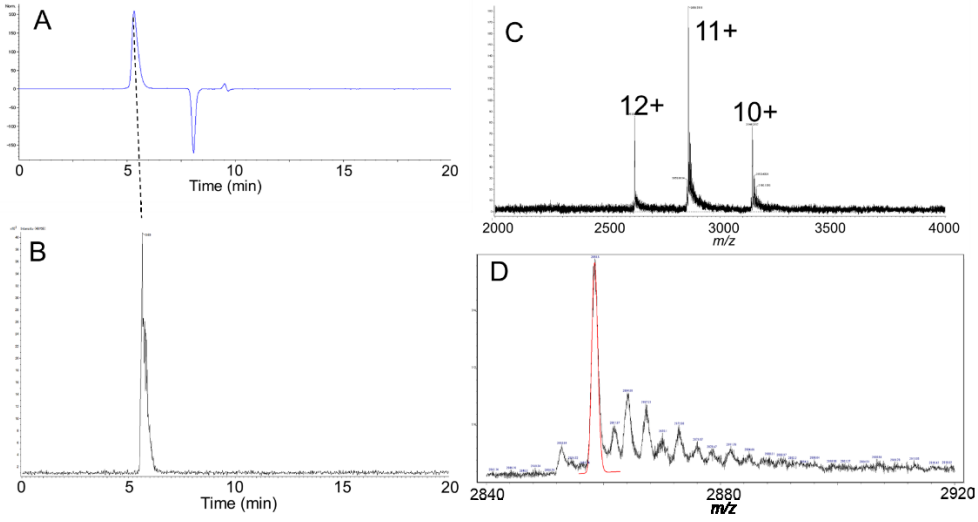

Fig. 3-5 (A) The UV spectrum and (B) TIC of bovine SOD-1 measured by SEC-ESI-MS, and the MS spectrum, the number was indicated charge states of the peaks. (D) Fitting of the peak (11+) of SOD-1 homodimer with Zn^{2+} ion and Cu^{2+} ion. Black line is observed peak and red line is theoretical peak. Observed m/z = 2858.51, and theoretical m/z = 2858.53.

Protein mixture sample, myoglobin, bSOD-1, and OVA, was measured by SEC-ESI-MS (Fig. 3-6). In this condition, each protein could not sufficiently separate by SEC, but they could be distinguished one another by their mass chromatograms.

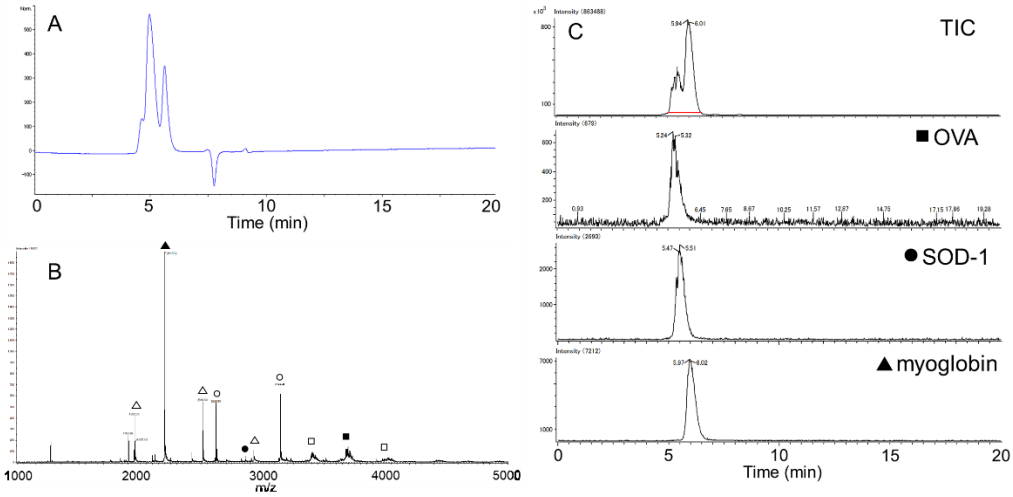

Fig. 3-6 (A) The UV spectrum (214 nm) of OVA, bSOD-1, and myoglobin mixture sample. (B) The MS spectrum from 5 – 7 min, and squares are OVA, circles are bSOD-1, and rectangle are myoglobin. (C) TIC and MS chromatograms of each protein, and MS chromatograms are integrated of MS peaks marked with closed shapes.

To check the quantification ability of SEC-ESI-MS, various amounts (25~ 200 pmol, n = 3) of myoglobin were measured, and the peak areas obtained from the UV (214 nm), TIC, and MS chromatograms at m/z,1952 (9+), 2196 (8+), and 2510 (7+) were plotted to make the standard curves (Fig. 3-7).

Not only UV standard curves, but also TIC and MS chromatograms showed the high linearity, where R^2 was more than 0.99 except for the peak of m/z = 1952 ($R^2 > 0.97$). This result shows that MS chromatogram can be used for the quantitative analysis. Especially, it has the advantages for the case that a protein mixture is not separated one another or a protein complex comprises of different constituents such as small compounds or metal ions as a ligand or co-factor, which are difficult to estimate by UV absorption. It could also allow for the stoichiometric analysis of the components of a complex. Although the present system has the above great merits, it has sometimes led to a breakdown of a complex during measurement, which owes to the relatively hard electrospray conditions (higher temperature and voltage on the cones) in comparison with the nanospray. Thus, it could be difficult to detect the “fragile” complex which comprises the

components weakly interacting each other. This issue could be partly solved by SEC, which gives the information on the sizes of analytes in solution.

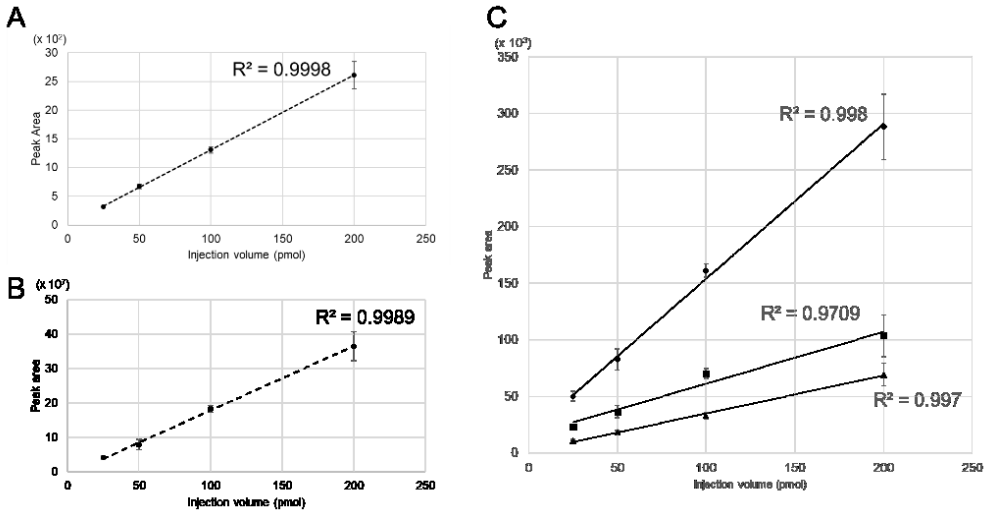

Fig. 3-7 Standard curves obtained with UV 214 nm (A), TIC (B), and MS chromatogram (C) obtained for myoglobin. the square shape is m/z 1952 (charge state; 9+), the diamond shape is m/z = 2196 (charge state; 8+), and the rectangle shapes is m/z = 2510 (charge state; 7+)

Analysis of the complex of RNase HI and RNA/DNA hybrid.

We found that some metal ion, most probably, Cu^{2+} ion, which could be eluted from stainless steel parts (pump, syringe needle, bulb, etc.) coordinated with RNase HI, which could make it active. As a result, RNA/DNA hybrid was partially hydrolyzed during SEC-ESI-MS measurement, giving RNase HI, RNA fragment, and DNA, as the result of hydrolysis, together with unaffected complex of RNase HI and RNA hybrid (Fig. 3-8).

To avoid the hydrolysis of RNA/DNA hybrid during separation, the bio-inert LC system was utilized. In addition, EDTA was added into the sample solution. As the result, the complex of RNase HI and RNA/DNA hybrids (1: 1 and 2: 1) was successfully detected (Fig. 3-9).

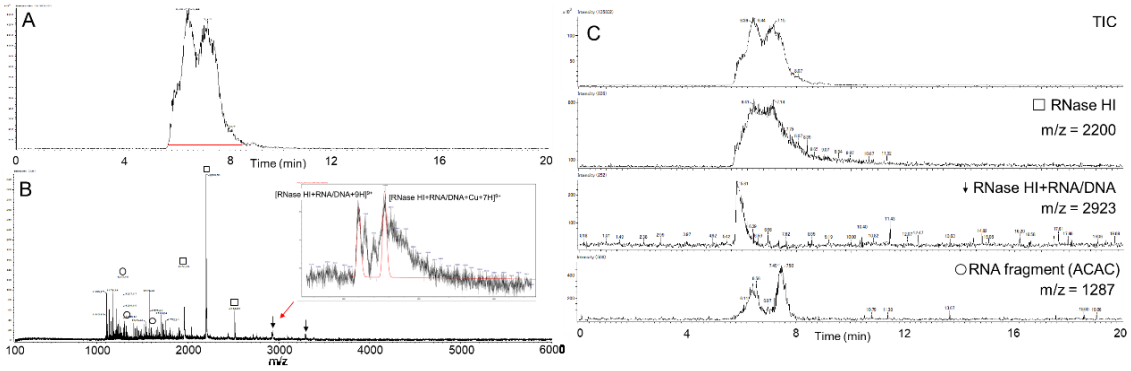

Fig. 3-8 (A) TIC of RNase HI and RNA/DNA 14-mer mixture solution (B) The MS spectrum from 5.5 – 8.6 min, and squares are RNase HI, circles are RNA fragments, m/z = 1592 (ACACC), 1305 (UGAU), and 1287 (ACAC), and arrows are 1:1 complex of RNase HI and RNA/DNA hybrid. (C) MS chromatograms of each peak.

The elution time of RNA/DNA hybrid was faster than RNase HI (Fig. 10), though the molecular weight was smaller than RNase HI, because the shape of RNA/DNA hybrid was not globular, but fibrous, thus, the elution time was retarded from those estimated for globular proteins. The peak corresponding to RNase HI was detected in wide time range, as it should be, in part, derived from the complex due to the decomposition of the complex during the process of vaporization and ionization. Note that heated nebulizer gas was used for getting fine spray which is indispensable for the ions being efficiently introduced into MS. From this point, the 1:1 complex, which was eluted at almost the same time as the 2:1 complex, was most likely to be produced by breakdown of the 2:1 complex.

SEC-ESI-MS allowed for detection of the complex of RNase HI and RNA/DNA hybrid, however, it needs to be set up with a metal-free (bio-inert) equipment such as LC pump, line, injector, etc. to avoid contamination of metal ions, which might have high propensity to bind to RNase HI to be the active form.

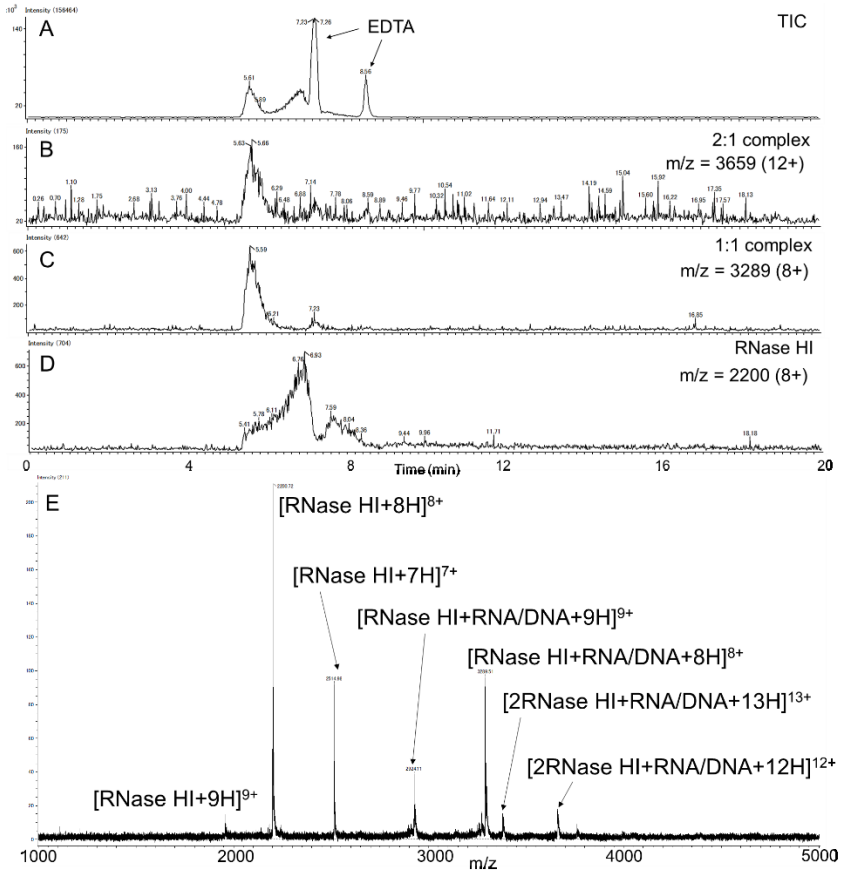

Fig. 9 TIC of RNase HI and RNA/DNA 14-mer mixture (A); MS chromatograms of m/z = 3659 (= 2:1 complex) (B); m/z = 3289 (= 1:1 complex) (C); m/z = 2200 (= RNase HI) (D); MS spectrum obtained by accumulation from 5.4 to 7.1 min in A (E).

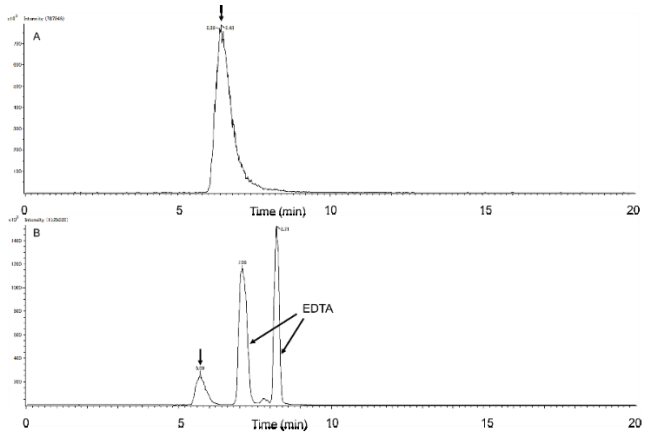

Fig.10 TIC of RNase HI (A); RNA/DNA hybrid 14-mer (B). The arrows showed each sample.

Analysis of human SOD-1.

Next, in order to demonstrate that the chemically synthesized and reconstituted human SOD-1 was folded correctly to incorporate the two divalent ions (Cu^{2+} and Zn^{2+}), it was subjected to SEC-ESI-MS. Human SOD-1 (hSOD-1) is a homodimer, each monomer of which coordinates one Cu^{2+} and one Zn^{2+} ion. The elution profile and retention time (Fig. 3-11) were similar to those of bovine SOD-1 (bSOD-1) observed in Figs. 3-5 and 3-6. In addition, the MS profile (Fig. 1-11C) predominantly showed the dimer. Thus, the synthetic hSOD-1 was found to be correctly synthesized and re-folded, as a homodimer, with four divalent ions ($2Cu^{2+}$ and $2Zn^{2+}$ ions) (Fig. 3-12). It should be noted that the monomer of hSOD-1was slightly observed in the spectrum, which was hardly observed for bSOD-1 (Fig. 3-5C), implying that the homodimer interaction of hSOD-1 was relatively weaker than bSOD-1, which should have been caused by the present electrospray conditions.

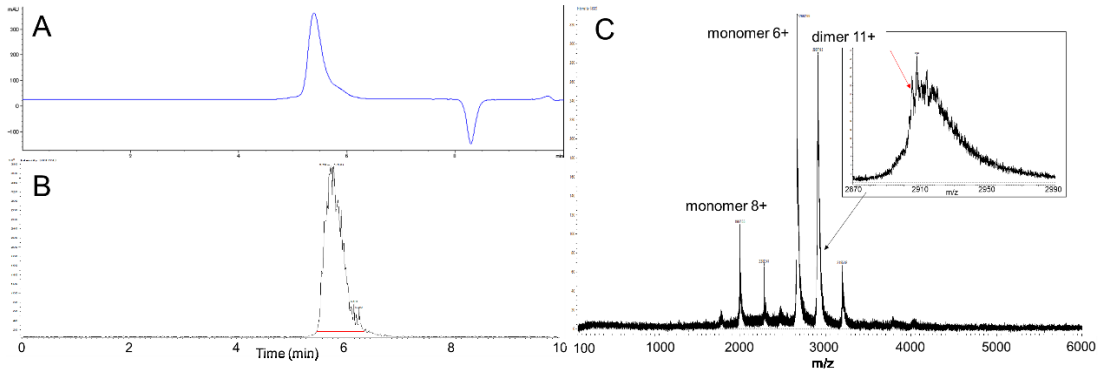

Fig. 3-11 (A)The UV chromatogram (214 nm) and (B) TIC of human SOD-1 with Cu^{2+} ion and Zn^{2+} ion by SEC-ESI-MS. (C) MS spectrum of human SOD-1 obtained from the peak underlined in red. The m/z value at 2904.8 indicated by a red arrow corresponds to the theoretical one (2904.6) of SOD homodimer coordinated with two Cu^{2+} ions and two Zn^{2+} ions. The slight difference in retention time between the UV and TIC was caused by the dead volume of the connecting tube in between the outlet of the UV cell and the top of the needle.

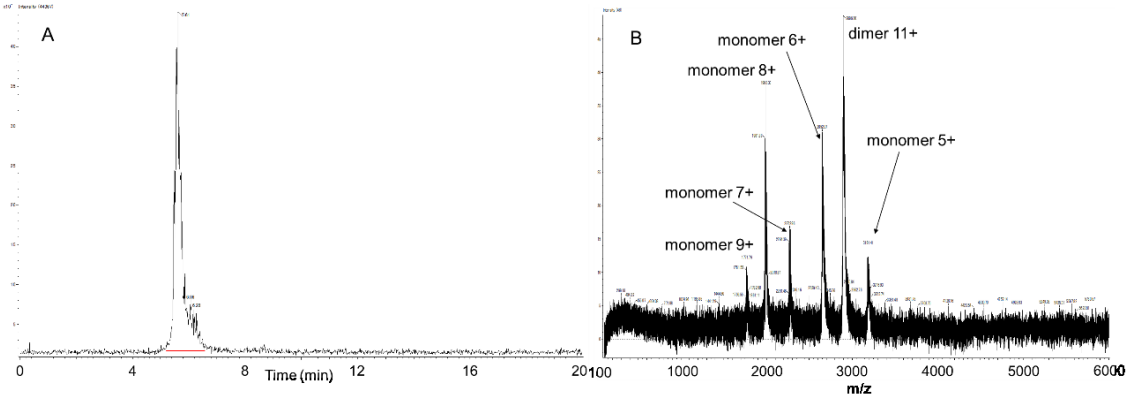

Fig.14 (A) TIC and (B) MS spectra of human SOD-1 without metal ions by SEC-ESI-MS.

3-4. Conclusion

This chapter showed that SEC-ESI-MS was a useful tool for analyzing a protein complex, by which the relative quantity of the complex and stoichiometry of the components could be revealed at the same time. It should be noted that the present measurement could be performed when the complex can be kept in volatile buffer with weaker ion strength such as 10 mM AcONH4, which has been generally used through the present work. Also, the LC system and ESI tip or probe should be metal-free, because a trace amount of metal ions could be coordinated with proteins in some specific manner. Meanwhile, the electrospray of the water-based buffer has often become unstable, causing deviation of TIC, which leads to poor quantification capability. To overcome this problem, the following settings and adjustments shall be important: 1) the flow rate of SEC should be optimized in relation to the diameter of the top of an ESI needle; 2) the voltage put on the capillary and the distance between the top of the capillary and the cone of the ES source should be optimized.

The noncovalent complex like SOD-1 (homodimer) and RNase HI (complex with the substrate RNA/DNA hybrid) could be measured time to time during separation with a SEC column, which enabled the detection of the slight different components or modified structures that could not be differentiated by SEC-UV. However, the applicability of the present SEC-ESI-MS to the analysis of complexes should be examined in advance with respect to the stability of a complex, indicated by such as a Kd value of the components comprising the complex.

Summary

Chapter 1: Detection of the complex of native *E.coli* RNase HI

The ternary complex of RNase HI, RNA/DNA hybrid, and Mn^{2+} ion, which has the enzymatic activity, could, for the first time, be detected by native MS. Although Mn^{2+} ion had low affinity to RNase HI in the absence of RNA/DNA hybrid, the ternary complex having two (not one) Mn^{2+} ions was transiently but specifically observed at 1.5 to 2 min after mixing these three components, which has the full enzymatic activity equivalent to the authentic enzyme.

Chapter 2: Characterization of RNase HI coordinated with Zn^{2+} ions

Zn^{2+} ion had a strong affinity to RNase HI in absence of RNA/DNA hybrids, which was not observed in the case of Mn^{2+}, and only one Zn^{2+} ion was associated with RNase HI, implying that RNase HI should have a specific Zn^{2+} binding site. It is interesting to speculate that nascent RNase HI after being expressed in a cell has already been associated with one Zn^{2+} ion, and then, with the second divalent ion such as Zn^{2+}, Mn^{2+}, or Mg^{2+} together with a substrate to hydrolyze the RNA chain.

The ternary complex with Zn^{2+} ion could be formed with the stoichiometry of RNase HI: RNA/DNA hybrid: Zn^{2+} = 1: 1: 2, which was the same as Mn^{2+} case. However, it is noteworthy that two Zn^{2+} -complex, observed in MS, was the ternary complex but with the hydrolyzed RNA. Since the reaction rate of Zn^{2+} -form was faster than Mn^{2+} -form, the active ternary complex before the reaction has not ever been observed. Nevertheless, it strongly supports that RNase HI functions with the two metal ions' catalysis.

Although the enzymatic activity was attenuated with higher concentration of Zn^{2+} ion (50 μM～), RNase HI exhibited 1.18-times higher activity than Mn^{2+} -complex, and moreover, at low concentration (1 μM) of Zn^{2+} ion, the activity increased 3.25-times high in comparison with that of Mn^{2+} -complex. Zn^{2+} ion might raise the stability of RNase HI itself or the complex, which was partly supported by observation of the ternary complex that retained the hydrolyzed RNA chain, which was released for the case of Mn^{2+} -complex.

These results suggest the new catalytic mechanism of RNase HI that needs to be elucidated by further studies with calorimetric, X-ray analyses, etc.

Chapter 3: Analysis of protein complexes using Size exclusion chromatography-electrospray ionization mass spectrometry

SEC-ESI-MS was a useful tool for analyzing a protein complex, by which the relative quantity of the complex and stoichiometry of the components could be revealed at the same time. It should be noted that the present measurement could be performed when the complex can be kept in volatile buffer with weaker ion strength such as 10 mM NH_4OAc, which has been generally used through the present work. Also, the LC system and ESI tip or probe should be metal-free, because a trace amount of metal ions could be coordinated with proteins in some specific manner. Meanwhile, the electrospray of the water-based buffer has often become unstable, causing deviation of TIC, which leads to poor quantification capability. To overcome this problem, the following settings and adjustments shall be important: 1) the flow rate of SEC should be optimized in relation to the diameter of the top of an ESI needle; 2) the voltage put on the capillary and the distance between the top of the capillary and the cone of the ES source should be optimized.

The noncovalent complex like SOD-1 (homodimer) and RNase HI (complex with the substrate RNA/DNA hybrid) could be measured time to time during separation with a SEC column, which enabled the detection of the slight different components or modified structures that could not be differentiated by SEC-UV. However, the applicability of the present SEC-ESI-MS to the analysis of complexes should be examined in advance with respect to the stability of a complex, indicated by such as a Kd value of the components comprising the complex.

Reference

1. Stein H, Hausen P., *Science.* **1969**, 166, 393–395.
2. Crouch, R. J. & Dirksen, M.-L. in Nuclease, eds. Linn, S. M., Roberts, R. J., 1982, 211-241.
3. Wintersberger, U., *Pharmacology and Therapeutics*,**1990** ,48(2),259–280.
4. Ohtani, N., Haruki, M., Morikawa, M., Kanaya, S., *Journal of Bioscience and Bioengineering*, **1999**, 8(1), 12–19.
5. Tadokoro, T., Kanaya, S., *FEBS J.*, **2009** ,276, 1482–1493
6. Kanaya, S., Crouch, R. J., *The Journal of Biological Chemistry*, 1983, 258(2), 1276–1281.
7. Itaya, M., *Proc. Natl. Acad. Sci.*, **1990**, 87, 8587-8591.
8. Kogoma, T., Foster, P. L., Ribonucleases H; Crouch R. J., Toulme, J. J., Eds., INSERM, Paris, **1998**, 39-66.
9. Turchi, J. J., Huang, L., Murante, R. S., Kim, Y., & Bambara, R. A., *Proceedings of the National Academy of Sciences of the United States of America*, **1994**, 91(21), 9803–7.
10. Aguilera, A., and Garcia-Muse, T., *Mol. Cell*, **2012**, 46, 115-124
11. K. Katayanagi, M. Miyagawa, M. Matsushima, M. Ishikawa, S. Kanaya, M. Ikehara, T. Matsuzaki, K. M., *Nature*, **1990**, 347(20), 306–310.
12. Yang, W., Hendrickson, W. a, Crouch, R. J., Satow, Y., *Science*, **1990**, 249, 1398–1405.
13. Katsuo Katayanagi, Mika Okumura, and K. M., *Proteins*, **1993**, 17(4), 337–346.
14. Goedken, E. R., Marqusee, S., *Journal of Biological Chemistry*, **2001**, 276(10), 7266–7271.
15. Davies, J. F., Hostomska, Z., Hostomsky, Z., Jordan, S. R., Matthews, D. A., *Science*, **1991**, 252(5002), 88–95.
16. Keck, J. L., Goedken, E. R., Marqusee, S., *The Journal of Biological Chemistry*, **1998**, 273(51), 34128–34133.
17. Steitz, T. A., & Steitz, J. A., *Proceedings of the National Academy of Sciences*, **1993**, 90(14), 6498–6502.
18. Black, C. B., & Cowan, J. A., *Inorganic Chemistry*, **1994**, 33(25), 5805–5808.
19. Nowotny, M., & Yang, W., *The EMBO Journal*, **2006**, 25(9), 1924–33.
20. Vivo, M. De, Peraro, M. D., & Klein, M. L., *J. Am. Chem. Soc.*, **2008**, 231(13), 10955–10962.
21. Nowotny, M., Yang, W., *The EMBO Journal*, **2006**, 25(9), 1924–33.
22. Nowotny, M., Gaidamakov, S. a, Crouch, R. J., Yang, W., Cell, **2005**, 121(7), 1005–16.
23. Nowotny, M., Gaidamakov, S. A., Ghirlando, R., Cerritelli, S. M., Crouch, R. J., Yang, W., *Molecular Cell*, **2007**, 28(2), 264–76.
24. Kay, L. E., *Journal of Magnetic Resonance,* **2005**, 173(2), 193–207.
25. Parker, M. W., *Journal of Biological Physics*, **2003**, 29(4), 341–362.

26. Bai, X. chen, McMullan, G., Scheres, S. H. W., *Trends in Biochemical Sciences*, **2015**, 40(1), 49–57.
27. Davis, A. M., Teague, S. J., & Kleywegt, G. J., *Angewandte Chemie - International Edition*, **2003**, 42(24), 2718–2736.
28. Lampe, J. N., *Frontiers in Pharmacology*, **2017**, 8(AUG).
29. Robert HH van den Heuvel, Heck, A. J. R. *Current Opinion in Chemical Biology*, **2004**, 8(5), 519–26.
30. Susa, A. C., Xia, Z., Williams, E. R., *Angewandte Chemie - International Edition,* **2017**, 56(27), 7912–7915.
31. Susa, A. C., Xia, Z., Williams, E. R., *Analytical Chemistry*, **2017**, 89, 3116−3122
32. Loo, J. a., Berhane, B., Kaddis, C. S., Wooding, K. M., Xie, Y., Kaufman, S. L., Chernushevich, I. V., *Journal of the American Society for Mass Spectrometry*, **2005**, 16, 998–1008.
33. Snijder, J., Rose, R. J., Veesler, D., Johnson, J. E., & Heck, A. J. R.,. *Angewandte Chemie - International Edition*, **2013**, 52(14), 4020–4023.
34. Olinares, P. D. B., Dunn, A. D., Padovan, J. C., Fernandez-Martinez, J., Rout, M. P., Chait, B. T., *Analytical Chemistry*, **2016**, 88(5), 2799–2807.
35. Muneeruddin, K., Thomas, J. J., Salinas, P. A., Kaltashov, I. A., *Analytical Chemistry*, **2014** 84(21), 10692–10699.
36. Bao, J., Krylova, S. M., Cherney, L. T., LeBlanc, J. C. Y., Pribil, P., Johnson, P. E., Wilson, D. J., Krylov, S. N., *Analytical Chemistry*, **2014**, 86(20), 10016–20.
37. Kanaya, S., & Crouch, R. J. *The Journal of Biological Chemistry*, **1982**, 258(2), 1276–1281.
38. Haruki, M., Noguchi, E., Akasako, A., Oobatake, M., Itaya, M., Kanaya, S. *Journal of Biological Chemistry*, **1994**, 269(43), 26904–26911.
39. Kimura, S., Nakamura, H., Hashimoto, T., Oobatake, M., Kanaya, S. *Journal of Biological Chemistry*, **1992**, 267, 21535–21542.
40. Kanaya, S., Kohara, A., Miura, Y., Sekiguchi, A., Iwai, S., Inoue, H., Ohtsuka E., Ikehara, M. The Journal of Biological Chemistry, **1990**, 265(8), 4615–4621.
41. Kashiwagi, T., Jeanteur, D., Haruki, M., Katayanagi, K., Kanaya, S., Morikawa, K. *Protein Engineering*, **1996**, 9(10), 857–67.
42. Itaya, M., & Crouch, R. J. *Molecular & General Genetics*, **1991**, 227(3), 424–432.
43. Kanaya, S., Oobatake, M., Nakamura, H., & Ikehara, M. *Journal of Biotechnology*, **1993**, 28(1), 117–136.
44. Kanaya, S., Oobatake, M., & Liu, Y. *Journal of Biological Chemistry*, 1996, 271(51), 32729–32736.
45. Uchiyama, Y., Iwai, S., Ueno, Y., Ikehara, M., Ohtsuka, E. *J. Biochem*., **1994**, 16, 1322–

1329.

46. Fenstermacher, K. J., DeStefano, J. J. J*ournal of Biological Chemistry*, **2011**, 286(47), 40433–40442.
47. Wang, D., Hurst, T. K., Thompson, R. B., Fierke, C. A. *Journal of Biomedical Optics*, **2011**, 16(8), 87011.
48. Kükrer, B., Filipe, V., Van Duijn, E., Kasper, P. T., Vreeken, R. J., Heck, A. J. R., Jiskoot, W. Pharmaceutical Research, **2010**, 27(10), 2197–2204.
49. Muneeruddin, K., Thomas, J. J., Salinas, P. A., Kaltashov, I. A. *Analytical Chemistry*, **2014**, 84(21), 10692–10699.
50. Haberger, M., Leiss, M., Heidenreich, A., Hafenmair, G., Hook, M., Bonnington, L., Wegele, H., Haindl, M., Reusch, D., Bulau, P., *mAbs*, **2016**, 8(2), 331–339.
51. Takei, T., Andoh, T., Takao, T. Hojo, H., *Angewandte Chemie International Edition*, **2017**, 1, 15708–15711.
52. Antonini, E., Brunori, M., *Hemoglobin and Myoglobin in their Reactions with Ligands*, **1971**, North-Holland Publishing Company, pp. 127

Acknowledgements

I wish to express my greatest gratitude to Professor Toshifumi Takao for a great number of invaluable suggestions, discussions, and hearty encouragement throughout this work. The whole work was carried out under his supervision in his laboratory (Laboratory of Protein profiling and functional proteomics) at Institute for Protein Research, Osaka University.

I would like to express my gratitude to Associate Professor Nobuaki Okumura for valuable suggestions and discussions.

I would like to express my gratitude to Professor Shigenori Kanaya from Graduate School of Engineering, Osaka University for the donation of *E. coli* RNase HI sample, valuable suggestions and discussions.

I would like to express my special thanks to the members of Takao Lab.

I am grateful for the financial support to Suntory Foundation For Life Sciences; “SUNBOR SCHOLARSHIP.”

I am also grateful to the financial support from Protein Research Foundation.

Finally, I am grateful to my family for their understanding, encouragement and support on this study.